

The Structure of Lipids and Proteins Studied by Attenuated Total Reflection (ATR) Infrared Spectroscopy

II. Oriented Layers of a Homologous Series: Phosphatidylethanolamine to Phosphatidylcholine

U. P. Fringeli

Laboratory for Physical Chemistry, Swiss Federal Institute of Technology, Zurich

(Z. Naturforsch. **32 c**, 20–45 [1977]; received November 15, 1976)

Infrared Dichroism, Structure of Phospholipids, Phosphatidylcholine,
Phosphatidylethanolamine Derivatives

Polarized infrared ATR spectra of dry oriented multilayers of dipalmitoylphosphatidylethanolamine, sheep brain phosphatidylethanolamine, dipalmitoylphosphatidyl-N-methylethanolamine, dipalmitoylphosphatidyl-N,N-dimethylethanolamine, dipalmitoylphosphatidylcholine and egg phosphatidylcholine are reported. Structural features of hydrocarbon chains and polar headgroups are discussed. The average deviation of hydrocarbon chains from the normal to the plane of the bilayer was found to be $20\text{--}30^\circ$. However it was not possible to decide whether the chains are oriented parallel to each other. The fatty acid ester groups in β - and γ -position have different conformations. The phosphate group of dipalmitoylphosphatidylethanolamine exists probably in the protonated ($\text{O}=\text{P}(\text{OH})$) and not in the ionized ($>\text{PO}_2^-$) state. However, the latter state is expected for all other phospholipids of this series. The deviation of the bisector of $\angle(\text{OPO})$ of the $>\text{PO}_2^-$ group from the normal to the bilayer is less than 45° and the mean orientation of all polar head groups is rather parallel than perpendicular to the plane of the bilayer. The polar headgroup of phosphatidylcholine assumes at least two different conformations of the $\text{O}-\text{C}-\text{C}-\text{N}$ moiety, *i. e. gauche* and *trans*. A variety of conformers has to be expected also for the polar head groups of most of the other phospholipids investigated in this work.

1. Introduction

Infrared (IR) spectra of a variety of phospholipids have been reported earlier by several authors^{1–4} and have served mainly for analytical purpose. More recently successful attempts have been made to get structural information from vibrational spectra^{5–7}. IR techniques become considerably more efficient when polarized infrared light is used⁸. Recently attenuated total reflection (ATR) spectroscopy with polarized light has turned out to be optimum for the study of oriented layer assemblies of lipids^{9–14}, proteins^{15, 16} and lipid-protein systems¹⁷.

Vibrational spectra of phospholipids may also be obtained via laser Raman spectroscopy which reveals in many cases information complementary to IR-spectroscopy. It was found that hydrocarbon transitions dominate the Raman spectra at the expense of those of the polar head group¹⁸. In IR-spectra, however, polar groups give rise to intensive absorption bands whereas C–C-stretching absorption bands are rather weak. Therefore, Raman spectroscopy was used to study phase transitions of hydrocarbon chains in phospholipids^{19, 20}.

In this paper we shall compare the molecular structure of dry oriented layers of α -L-dipalmitoylphosphatidylethanolamine (DPPE), α -L-dipalmitoylphosphatidylmonomethylethanolamine (DPPME), α -L-dipalmitoyl-phosphatidylidemethylethanolamine (DPPDME), α -L-dipalmitoyl-phosphatidylcholine (DPPC), sheep brain phosphatidylethanolamine (sh.br.PE) and egg phosphatidylcholine (egg-PC).

2. Experimental

2.1. ATR-Spectra

For a general review of ATR-technique the reader is referred to reference²¹.

The ATR-spectra were recorded on a Perkin Elmer Mod. 225 infrared spectrometer equipped with two ATR attachments (Wilks Sci. Corp., Mod. 9 and Mod. 50). The reflection plates were germanium, KRS-5 or zinc selenide ($50 \times 20 \times 1 \text{ mm}$) supplied by Harrick Sci. Corp. The angle of incidence was 30° for Ge and 45° for KRS-5 and

Requests for reprints should be sent to U. P. Fringeli, Laboratory for Physical Chemistry, Swiss Federal Institute of Technology, CH-8092 Zurich, Switzerland.



Dieses Werk wurde im Jahr 2013 vom Verlag Zeitschrift für Naturforschung in Zusammenarbeit mit der Max-Planck-Gesellschaft zur Förderung der Wissenschaften e.V. digitalisiert und unter folgender Lizenz veröffentlicht: Creative Commons Namensnennung-Keine Bearbeitung 3.0 Deutschland Lizenz.

Zum 01.01.2015 ist eine Anpassung der Lizenzbedingungen (Entfall der Creative Commons Lizenzbedingung „Keine Bearbeitung“) beabsichtigt, um eine Nachnutzung auch im Rahmen zukünftiger wissenschaftlicher Nutzungsformen zu ermöglichen.

This work has been digitized and published in 2013 by Verlag Zeitschrift für Naturforschung in cooperation with the Max Planck Society for the Advancement of Science under a Creative Commons Attribution-NoDerivs 3.0 Germany License.

On 01.01.2015 it is planned to change the License Conditions (the removal of the Creative Commons License condition "no derivative works"). This is to allow reuse in the area of future scientific usage.

ZnSe. This geometry results in ~ 40 and ~ 25 active internal reflections respectively. The reflection plates were thermostated to $\pm 0.5^\circ\text{C}$. Polarization measurements were made by means of a Perkin Elmer grid polarizer. A schematic set up of the ATR geometry used is shown in Fig. 1.

2.2. Preparation of oriented phospholipid layers

The phospholipid was dissolved ($\sim 10^{-3}\text{ M}$) in chloroform. A drop of the solution ($\sim 50\text{ }\mu\text{l}$) was put on one side ($\sim 10\text{ cm}^2$) of a ATR reflection plate. Now a small teflon bar was placed on the plate in such a way that the drop spread by capillary action between the ATR-plate and the bar. Slowly moving the bar along the plate for several times until the solvent had evaporated lead to multilayer formation. Homogeneity of the sample can be checked by observing interference colours. For instance, egg PC spread on a Ge surface gave a homogeneously yellow-brownish film over the entire surface corresponding to a mean thickness of 4–6 bilayers¹⁴. It should be mentioned that DPPE showed quite a different behaviour than the other phospholipids investigated. First its solubility in chloroform was much smaller and second no interference colours could be observed after evaporation of the solvent because sudden crystallization into microcrystals occurred leading to a opaque surface.

2.3. Chemicals

All synthetic phospholipids and amines obtained from Fluka AG, Buchs/SG, Switzerland, were of puriss grade. Sheep brain phosphatidyl ethanolamine was obtained from SIGMA London, Kingston-upon-Thames, England.

3. Orientation Measurements

3.1. Polarized ATR measurements

In studying oriented layers, ATR technique allows measurements with polarized radiation in a fairly straightforward way. Fig. 1 depicts schematically the experimental set up. If the incident radiation is \parallel (\perp) polarized, the probe field in the rarer medium is x, z (y) polarized. More explicitly: the field amplitudes in the rarer medium are approximated in the case of weak absorption for thin layers by²¹:

$$\begin{aligned} E_{y0} = E_{\perp} &= \frac{2 \cos \vartheta}{(1 - n_{31}^2)^{\frac{1}{2}}} \\ E_{x0} &= \frac{2 \cos \vartheta (\sin^2 \vartheta - n_{31}^2)^{\frac{1}{2}}}{(1 - n_{31}^2)^{\frac{1}{2}} [(1 + n_{31}^2) \sin^2 \vartheta - n_{31}^2]^{\frac{1}{2}}} \quad (1) \\ E_{z0} &= \frac{2 \cos \vartheta n_{32}^2 \sin \vartheta}{(1 - n_{31}^2)^{\frac{1}{2}} [(1 + n_{31}^2) \sin^2 \vartheta - n_{31}^2]^{\frac{1}{2}}}, \end{aligned}$$

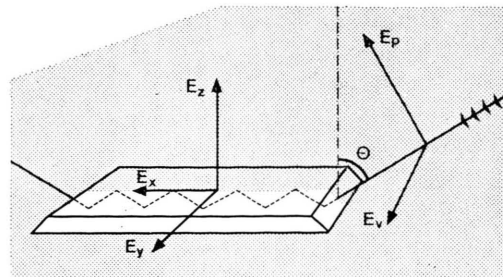


Fig. 1. ATR set up. ϑ : angle of incidence. E_p , E_v : parallel and perpendicular polarized components of the electric field of incident light. E_x , E_y , E_z : electric field components with respect to the coordinate system corresponding to the internal reflection plate ($E_p \rightarrow E_x$, E_z ; $E_v \rightarrow E_y$). (From ref. 11.)

n_{ik} denotes the ratio of refractive indices n_i/n_k of medium i and k. Indices 1, 2 and 3 stand for ATR plate, thin film and surrounding medium, respectively. For a bulk rarer medium index 3 must be replaced by 2. The total electric field amplitudes for parallel (\parallel , pp) and perpendicular (\perp , vp), polarization are given by

$$\begin{aligned} E_{\parallel} &= (E_x^2 + E_z^2)^{\frac{1}{2}} \\ E_{\perp} &= E_y. \end{aligned}$$

Molecular orientation is determined via the measurement of the dichroic ratio R which is defined as the ratio of the absorption coefficients of \parallel (pp) and \perp (vp) polarized light, respectively. R is given by

$$\begin{aligned} R &= \frac{A_{\parallel}}{A_{\perp}} = \frac{\int_0^{\infty} \ln T_{\parallel}(\tilde{\nu}) d\tilde{\nu}}{\int_0^{\infty} \ln T_{\perp}(\tilde{\nu}) d\tilde{\nu}} \quad (2) \\ &= \frac{|\mathbf{E}_{\parallel}|^2 |(\partial \mu | \partial Q)_0|^2 \cdot \cos^2(\mathbf{E}_{\parallel}, (\partial \mu | \partial Q)_0) *}{|\mathbf{E}_{\perp}|^2 |(\partial \mu | \partial Q)_0|^2 \cos^2(\mathbf{E}_{\perp}, (\partial \mu | \partial Q)_0)} \end{aligned}$$

where A denotes the integrated absorption coefficient and $T(\tilde{\nu})$ the transmission at the wavelength $\tilde{\nu}$. $(\partial \mu | \partial Q)_0$ denotes the derivative of the dipole moment with respect to the Q -th normal coordinate, *i.e.* the “oscillating dipole moment” or “transition dipole moment”²². For membrane layers the molecular orientation is not random. Experience shows that most often one of the molecular axis is symmetrically distributed around one space fixed direction enclosing an angle γ . Moreover in many cases

* For non-overlapping absorption bands the integrated absorption coefficients may be replaced by the peak absorption coefficients²⁴.

the oscillating dipole moment deviates by an angle Θ from the molecular axis and is cylindrically distributed with respect to the latter. Taking the z -axis as the space fixed direction one gets for the dichroic ratio:

$$R_z^{\text{ATR}} = \frac{E_x^2}{E_y^2} + \frac{E_z^2}{E_y^2} \frac{2 \cos^2 \Theta + S}{\sin^2 \Theta + S}. \quad (3)$$

The reader is referred to references^{23, 24} for details of the derivation which, however, relates to the case of transmission IR spectroscopy. Extension to ATR is straightforward. It is customary to introduce the order parameter S , defined by

$$S = \frac{F}{N - 3/2 F} \quad (4)$$

where

$$F = \langle \sin^2 \gamma \rangle = \int_0^{\pi/2} \sin^2 \gamma f(\gamma) d\gamma,$$

$$N = \langle f(\gamma) \rangle = \int_0^{\pi/2} f(\gamma) d\gamma = 1,$$

$f(\gamma)$ stands for the first density of the distribution of the angle γ . Model distributions $f(\gamma)$ have been discussed in references^{23–25}. The order parameter S becomes zero for perfect ordering and infinity for random distribution. For the sake of comparison it should be mentioned that the parameter S' generally used in EPR and NMR spectroscopy is defined by

$$S' = 3/2 \int_0^{\pi/2} \cos^2 \gamma f(\gamma) d\gamma - 1/2. \quad (5)$$

S' becomes unity for perfect ordering and zero for random distribution. However, expression (6) relates (5) to (4)

$$S' = 1 - \frac{3/2 S}{1 + 3/2 S}. \quad (6)$$

3.2. Ultrastructure of samples

Two types of ultrastructure of the oriented layer systems discussed in this paper will turn out to be of importance:

(i) Microcrystalline ultrastructure: (MCU)

The layer is composed of submicroscopic domains each of which is characterized by fixed values of the polar angles γ and φ of the molecular orientation with respect to the coordinate system depicted in Fig. 1. The ensemble is described by a

fixed value of γ_0 and an isotropically distributed angle φ , *i.e.* isotropic molecular arrangement around the z -axis.

The distribution function is then given by:

$$f(\gamma) = \delta(\gamma - \gamma_0). \quad (7)$$

Fig. 2 gives the relation between the ATR dichroic ratio R_z^{ATR} and the angle γ_0 between the molecular axis and the z -axis for MCU type layer systems ($\Theta = 0$).

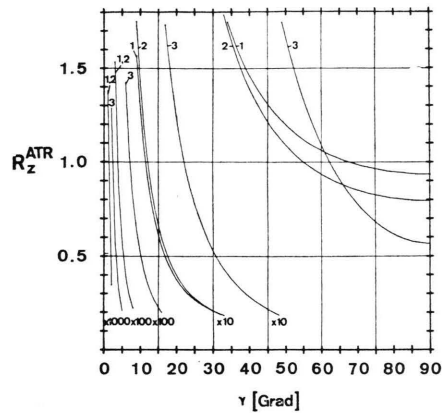


Fig. 2. Relationship between ATR-dichroic ratio R_z^{ATR} and angle γ between the molecular axis and the z -axis for oriented layers with microcrystalline ultrastructure (MCU-type, *cf.* Section 3.2). Calculation is based on (3) and (4) with $f(\gamma) = \delta(\gamma - \gamma_0)$. The angle of incidence was 45°.
 1: $n_1 = 4.0$ (germanium), $n_2 = 1.55$ (lipid), $n_3 = 1.0$ (air).
 2: $n_1 = 2.4$ (zinc selenide)*, $n_2 = 1.55$ (lipid), $n_3 = 1.0$ (air).
 3: $n_1 = 2.4$ (zinc selenide)*, $n_2 = 1.55$ (lipid), $n_3 = 1.33$ (water).

* Or KRS-5, or CdTe.

(ii) Liquid crystalline ultrastructure: (LCU)

The layer is an ensemble of molecules whose long molecular axis features a narrow distribution with respect to γ and an isotropic distribution with respect to φ . The model distribution function proposed by Kratky^{23–25} may be applied to LCU-type systems²⁶. It is defined by

$$f(\gamma) = \frac{v^{3/4} \sin \gamma}{(v^{-3/2} \cos^2 \gamma + v^{3/2} \sin^2 \gamma)^{3/2}} \quad (8)$$

where v denotes the extension ratio, describing the degree of ordering. $v = 1$ means isotropic and $v = \infty$ perfect molecular orientation, respectively. An application to unsaturated hydrocarbon chains of egg-PC is given in Fig. 11.

4. Results and Discussion

4.1. Crystallinity of samples

Decreasing crystallinity in the polar part of the molecules with increasing number of N-methyl groups is a typical feature of this homologous series. This behaviour is clearly shown by the varying half-width of typical absorption bands. Crystalline substances generally exhibit very sharp absorption bands. Strong polarization effects may occur. In the liquid crystalline state, however, the molecules may assume different conformations leading to considerably broader absorption bands and reduced polarization. All samples of α -L-dipalmitoyl-phosphatidylethanolamine (DPPE) exhibit microcrystallinity (MCU-type). It should be noted that on the hydrophobic surface of a KRS-5 ATR plate crystallization was more perfect (Fig. 3) than on the hydrophilic Ge surface (Fig. 4). The

N-methyl (DPPME) and the N,N-dimethyl (DPPDME) compounds may also recrystallize from a "liquid" crystalline to a solid crystalline state, *i.e.* the number of different conformations of the polar headgroup is reduced. In analogy to DPPE this often occurs when the multilayers are prepared on a hydrophobic surface such as KRS-5 (a tellurium bromide iodide compound) or zinc selenide, as shown by Figs 7 and 8.

Similar recrystallization phenomena have been observed with Langmuir-Blodgett type oriented layers of Ba-stearate and tripalmitin¹¹.

4.2. Structure of hydrocarbon chains

Saturated normal hydrocarbon chains in *all-trans* conformation exhibit characteristic sequences of absorption bands, *i.e.* the wagging progression ($\gamma_w(CH_2)$), twisting progression ($\gamma_t(CH_2)$),

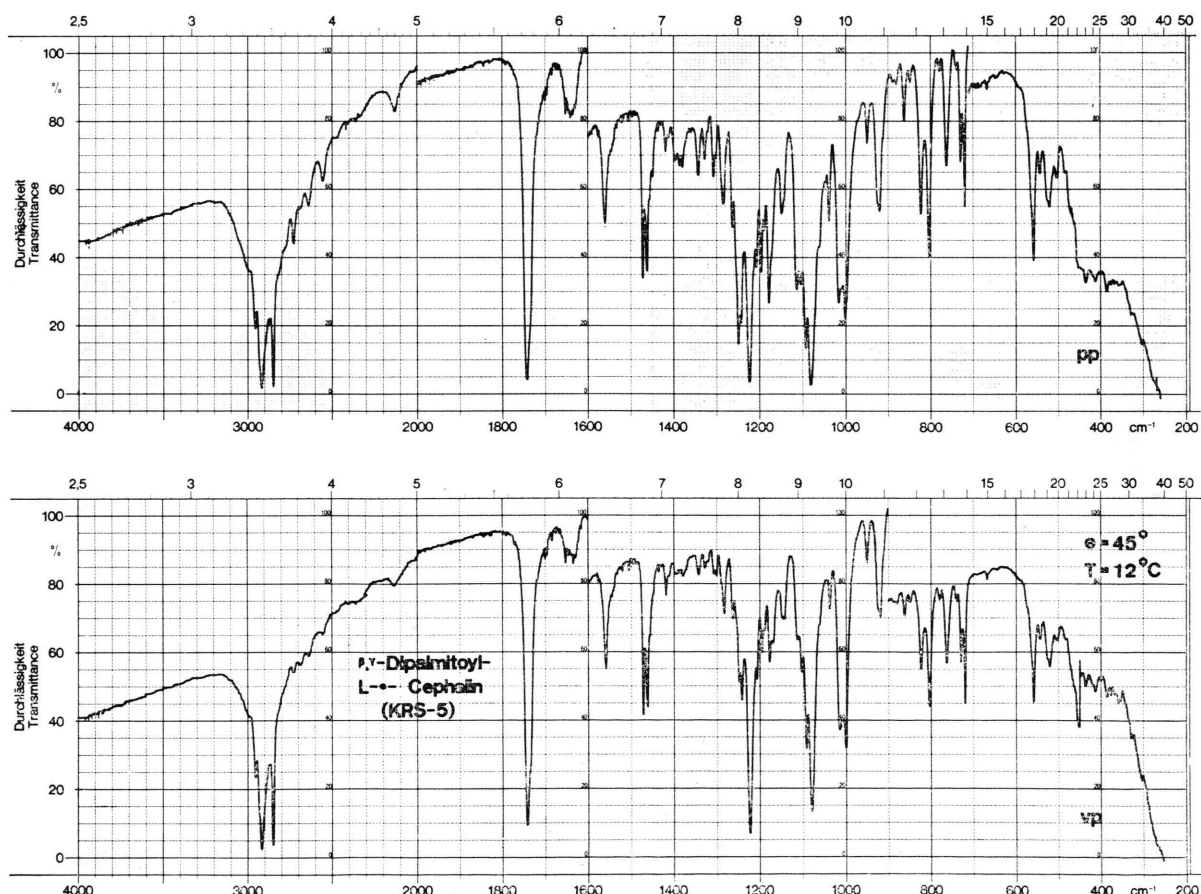


Fig. 3. Oriented layers of β,γ -dipalmitoyl-L- α -phosphatidylethanolamine (DPPE) on KRS-5 ATR plate. pp: parallel polarized, vp: perpendicular polarized, $\theta=45^\circ$, $T=12^\circ\text{C}$, rel. humidity <1%.

C–C-stretching progression ($\nu(C-C)$) and rocking progression ($\gamma_r(CH_2)$). These vibrations have been investigated by several workers^{27–31}. The intensity of the wagging progression depends strongly on the nature of the end group of the corresponding hydrocarbon chain. In *n*-alkanes $\gamma_w(CH_2)$ -bands have low intensity, whereas polar



end groups such as $-COOH$ or $-C-OR$ increase their intensity considerably. This is due to coupling of $\gamma_w(CH_2)$ modes with a vibration of the polar group, which increases the oscillating dipole moment, *i.e.* the intensity of the absorption band. Deviations of the hydrocarbon chain conformation from *all-trans* were found to lead to marked alterations in the wagging progression such as loss of intensity, band broadening, and finally disappear-

ance of the progression¹⁰. However little quantitative information is available at present about the behavior of the typical $\gamma_w(CH_2)$ -, $\gamma_t(CH_2)$ -, a.s.o. sequences of a given CH_2 -chain on the position and number of *gauche*-type defects. In case of paraffins studies of this type have been reported by Snyder³². Since the oscillating dipole moment of $\gamma_w(CH_2)$ is directed parallel to the chain, polarization measurements with the wagging progression is an efficient tool to determine the mean direction of *all-trans* hydrocarbon chains. However, deviation of the direction of the oscillating dipole from the hydrocarbon chain may be induced by certain polar end groups. In stearic acid for instance it was found that the deviation between chain and oscillating dipole moment is $\sim 30^\circ$ ³³. There are, however, no indications for a significant deviation in the case of triglycerides¹⁰ and phospholipids except DPPE.

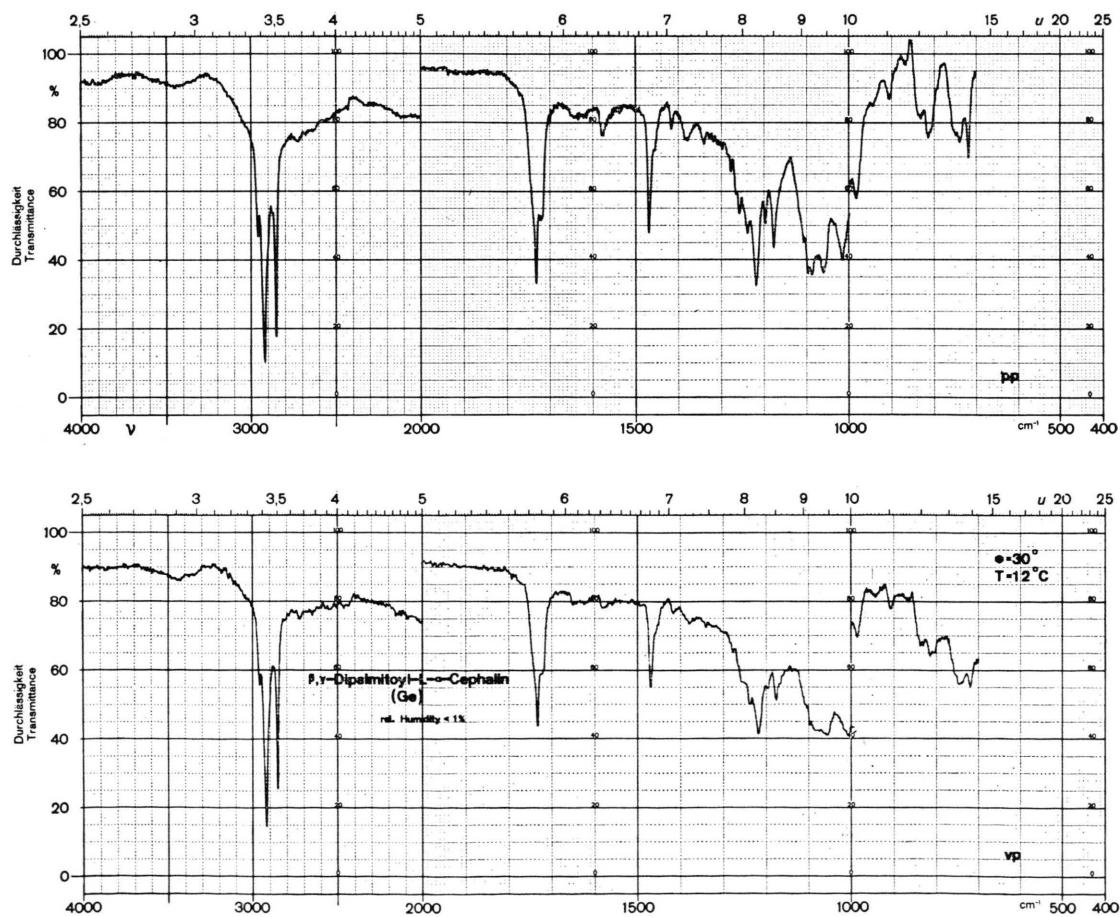


Fig. 4. Oriented layers of β, γ -dipalmitoyl-L- α -phosphatidylethanolamine on a germanium ATR-plate. pp: parallel polarized, vp: perpendicular polarized, $\vartheta=30^\circ$, $T=12^\circ C$, rel. humidity $< 1\%$.

Table I. Direction of hydrocarbon chains in oriented phospholipid multilayers with respect to the plane of the bilayers^a.

Substance b	R_z^{ATR} c	Φ_0 d	Comments			
Tripalmitin	4.0–4.5	71°–73°	Ge-ATR-plate,	$\vartheta=30^\circ$,	$T=26^\circ\text{C}$,	0% rel. humidity
DPPE	2.4–3.0	63°–67°	Ge-ATR-plate,	$\vartheta=30^\circ$,	$T=12^\circ\text{C}$,	0% rel. humidity
DPPME	1.9–3.4	59°–68°	KRS-5-ATR-plate,	$\vartheta=45^\circ$,	$T=15^\circ\text{C}$,	0% rel. humidity
DPPDME	2.3–2.6	62°–65°	KRS-5-ATR-plate,	$\vartheta=45^\circ$,	$T=22^\circ\text{C}$,	0% rel. humidity
DPPC	1.9–2.2	57°–61°	CdTe-ATR-plate,	$\vartheta=45^\circ$,	$T=22^\circ\text{C}$,	0% rel. humidity
Lysolecithin	4.7–6.9	71°–76°	KRS-5-ATR-plate,	$\vartheta=45^\circ$,	$T=22^\circ\text{C}$,	0% rel. humidity
Lysolecithin-OD	6.9–8.0	76°–78°	Ge-ATR-plate,	$\vartheta=45^\circ$,	$T=21^\circ\text{C}$,	0% rel. humidity

a A microcrystalline ultrastructure (MCU-type) is assumed, cf. Fig. 2.

b For explanation of the abbreviations cf. section 1

c ATR-dichroic ratio of the $\gamma_w(\text{CH}_2)$ band near 1200 cm^{-1} , cf. section 4.2.

d Angle between hydrocarbon chains and the plane of the bilayers.

For MCU-type ultrastructure of the homologous series DPPE to DPPC the mean angle between the hydrocarbon chains and the z -axis can be calculated by means of Eqs (3), (4), and (7). Values related

to this series as well as to tripalmitin and α -L-palmitoyl-lysophosphatidylcholine (Lysolecithin) are listed in Table I. Further information about the orientation of the hydrocarbon chains can be obtained by

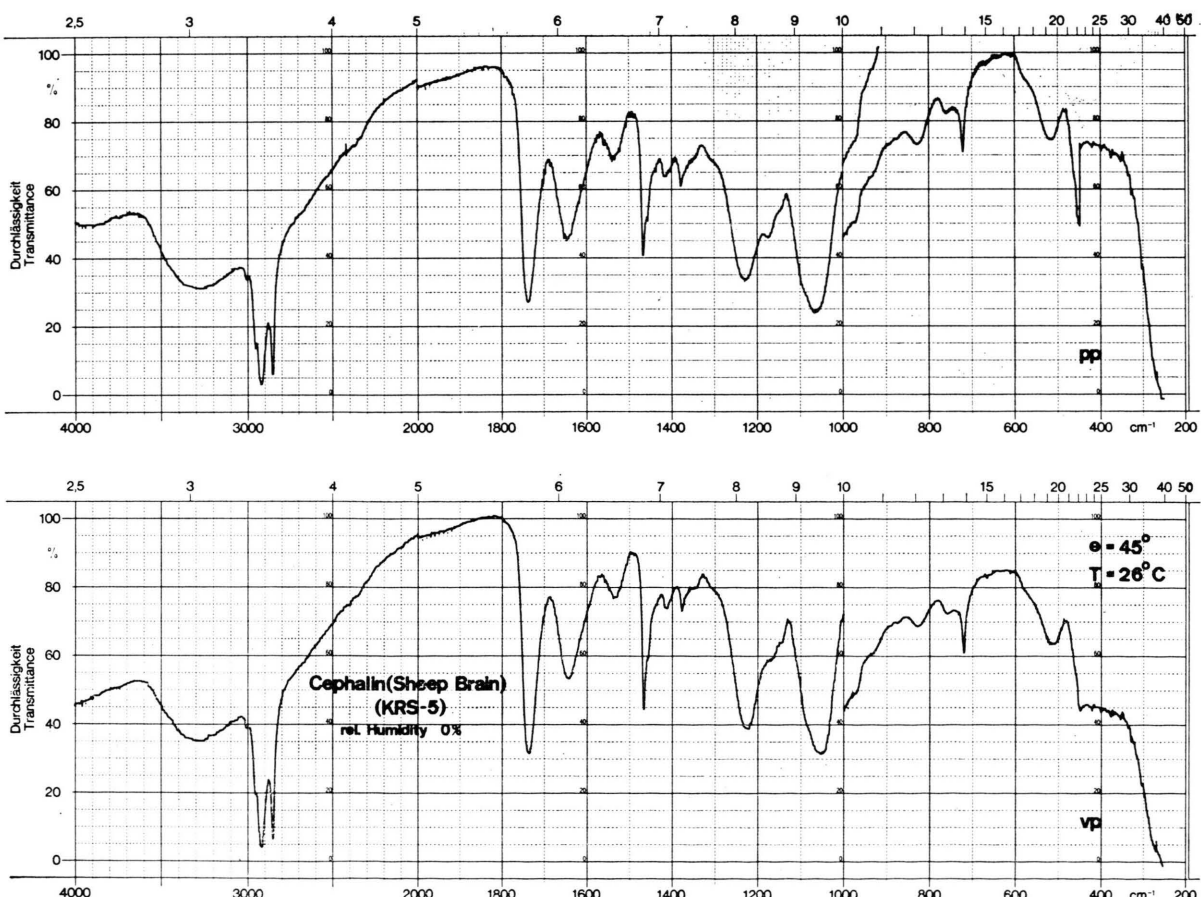


Fig. 5. Oriented layers of phosphatidylethanolamine (Sh.br.PE) from sheep brain on a KRS-5 ATR plate. pp: parallel polarized, vp: perpendicular polarized, $\vartheta=45^\circ$, $T=26^\circ\text{C}$, rel. humidity $<1\%$.

polarization measurements using CH_2 -bending ($\delta(\text{CH}_2)$, $\sim 1470 \text{ cm}^{-1}$) and symmetric and anti-symmetric CH_2 -stretching ($\nu_s(\text{CH}_2)$, $\sim 2850 \text{ cm}^{-1}$, $\nu_{as}(\text{CH}_2)$, $\sim 2920 \text{ cm}^{-1}$) vibrations. The oscillating dipole moments of both $\nu_s(\text{CH}_2)$ and $\delta(\text{CH}_2)$ is expected to lie along the bisector to $\angle(\text{HCH})$. Unfortunately the experimental error of the dichroic ratios of the two bands is rather high because of overlapping with CH -vibration bands of the polar part of the molecule. This handicap may be eliminated when the CH_2 -rocking ($\gamma_r(\text{CH}_2)$) band at 720 cm^{-1} is used, which in case of DPPC and lysolecithin is only weakly overlapped by the totally symmetric $\text{C}-\text{N}$ -stretching absorption band^{13, 56}. The transition moment of $\gamma_r(\text{CH}_2)$ is perpendicular to the plane of the C -atoms of the hydrocarbon chain. The angle Φ' between this direction and the plane of the bilayer may be determined from the

corresponding dichroic ratio (cf. Sec. 3). Using Φ' and Φ_0 (angle between hydrocarbon chain and plane of the bilayer, cf. Table I) one may calculate the angle α which denotes the rotation of the *all-trans* hydrocarbon chain about its long axis. $\alpha=0$ means that the $-\text{C}-\text{C}-\text{C}-$ plane is parallel to the z -axis.

Thus one obtains the following expression in case of $\gamma_r(\text{CH}_2)$:

$$\sin^2 \alpha = \frac{1 - \cos^2 \Phi'}{1 - \sin^2 \Phi_0}, \quad (9)$$

$\sin \alpha$ has to be replaced by $\cos \alpha$ if the $\nu_s(\text{CH}_2)$ or $\delta(\text{CH}_2)$ absorption bands are used.

Obviously one can determine only the mean rotation angle $\bar{\alpha}$ of both hydrocarbon chains (except for lysolecithin). Nevertheless $\bar{\alpha}$ may be used to compare a series of lipids with respect to their hydro-

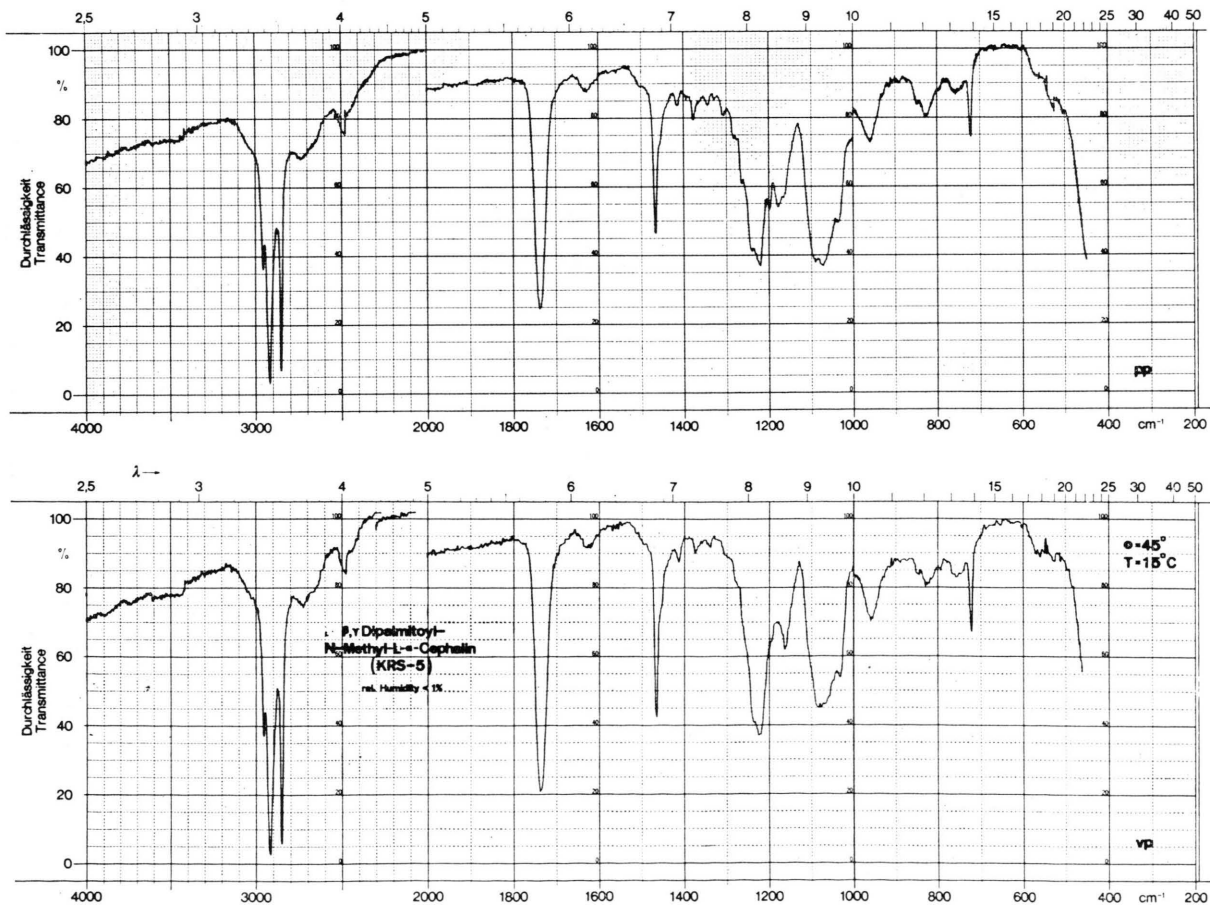


Fig. 6. Oriented layers of β,γ -dipalmitoyl-N-methyl-L- α -phosphatidylethanolamine (DPPME) on a KRS-5 ATR-plate. pp: parallel polarized, vp: perpendicular polarized, $\theta=45^\circ$, $T=15^\circ\text{C}$, rel. humidity $<1\%$.

carbon chain structures. The results of this investigation are summarized in Table II. They clearly demonstrate that DPPE and recrystallized lysolecithin show quite a different behaviour than the other compounds. Corresponding $\bar{\alpha}$ values of the former can not be calculated ($\sin^2 \alpha > 1$!), because the experimentally determined dichroic ratios are not consistent with the spectroscopic model used in this work, *i.e.* the assumption that intermolecular interactions may be observed as weak perturbations of the spectrum resulting from an isolated molecule.

The $\gamma_w(\text{CH}_2)$ progression vanishes above the transition temperature T_c , *i.e.* information about chain ordering (conformation and direction) from wagging absorption bands is lost. However, it has been recently shown that in the liquid crystalline state the mean order parameter of hydrocarbon

chains can still be determined by means of polarized infrared measurements of other hydrocarbon chain group vibrations, *e.g.* $\nu_{as}(\text{CH}_2)$, $\nu_s(\text{CH}_2)$, $\delta(\text{CH}_2)$, $\delta_s(\text{CH}_3)$ and $\nu(\text{C}-\text{C})$ ²⁶. Since most naturally occurring lipids contain unsaturated hydrocarbon chains typical double bond group vibrations may be used as natural probes to monitor hydrocarbon chain ordering. For a comprehensive summary of double bond group vibrations the reader is referred to Bellamy³⁴. The $\text{C}=\text{C}$ stretching vibration is expected to absorb in the 1620 to 1680 cm^{-1} range with variable intensity. α -L-1-palmitoyl-2-palmitoleoylphosphatidylcholine shows a weak absorption band near 1660 cm^{-1} . In egg phosphatidylcholine however, a prominent absorption band appears at 1610 cm^{-1} . Enhanced intensity and shift may result from conjugation with a second $\text{C}=\text{C}$ double bond³⁴, this, however, can be excluded in the case

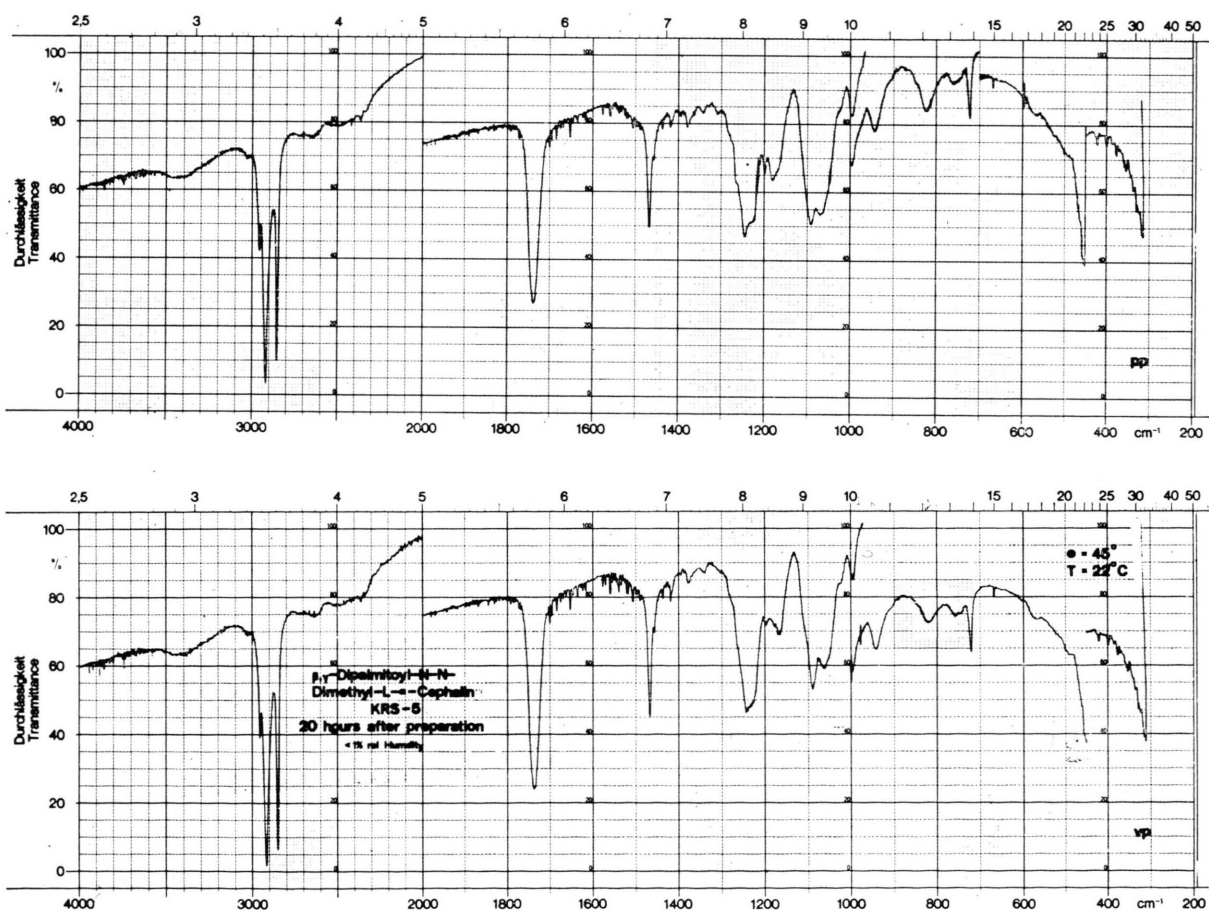


Fig. 7. Oriented layers of β,γ -dipalmitoyl-N,N-dimethyl-L- α -phosphatidylethanolamine (DPPDME) on a KRS-5 ATR plate. pp: parallel polarized, vp: perpendicular polarized, $\theta = 45^\circ$, $T = 22^\circ\text{C}$, rel. humidity $< 1\%$.

Table II. Mean angle $\bar{\alpha}$ between the $-\text{C}-\text{C}-\text{C}-$ planes of the hydrocarbon chains (*all-trans*) and the plane formed by the z -axis and the mean direction of the hydrocarbon chains ^a.

Substance ^b	R_{ATR} ^c	$\bar{\phi}'$ ^d	$\bar{\alpha}$ ^e	Comments
DPPE	1.53	52°	NC	Fig. 4, derived from $\delta(\text{CH}_2)$
DPPE (recryst.)	1.16, 1.05	44°, 39°	NC	Fig. 3, $\gamma_w(\text{CH}_2)$ doublet
DPPME	0.79	0°	~0°	Fig. 6
DPPDME	0.85	20°	46°–54°	Fig. 7
DPPC	0.94	26°	53°–64°	Fig. 9
DPPC-d9	0.85	0°	~0°	Fig. 17
lysolecithin	0.78	0°	~0°	KRS-5, $\vartheta=45^\circ$, $T=11^\circ\text{C}$, rel. humidity <1%
lysolecithin (recryst.)	1.64	36°	NC	Ge, $\vartheta=45^\circ$, $T=21^\circ\text{C}$, rel. humidity <1%

^a Derived from CH_2 -rocking [$\gamma_r(\text{CH}_2)$] band at 720 cm^{-1} because of minimum overlapping with other bands. Microcrystalline ultrastructure (MCU), *cf.* Secs. 3.2, 4.2 and 5.5. The transition moment of $\gamma_r(\text{CH}_2)$ is perpendicular to the $-\text{C}-\text{C}-\text{C}-$ plane.

^b For explanation of the abbreviations *cf.* Sec. 1.

^c ATR dichroic ratio, *cf.* Eqn (3).

^d Angle between average transition moment and the plane of the bilayer.

^e Mean rotation angle of the hydrocarbon chains, NC: not consistent with the model, *cf.* Sec. 5.6.

of natural phospholipids since multiple double bonds are generally separated by one CH_2 group, *e.g.* 9,12-octadecadienoic or 9,12,15-octadecatrienoic acid derivatives. Up to 6 double bonds per hydrocarbon chain have been found in certain phospholipids, the first one being in C-4 position ³⁵. Nevertheless band shift and intensity of $\nu(\text{C}=\text{C})$ in egg phosphatidylcholine could result from coupled stretching vibrations of single and double bonds. Furthermore the antisymmetric C–H stretching vibration $\nu_{\text{as}}(\text{CH})$ at 3008 cm^{-1} should be mentioned. For *cis*-double bonds the oscillating dipole moment may be expected to be parallel to the $\text{C}=\text{C}$ double bond. This band of medium or weak intensity may be overlapped by N-methyl CH –

stretching or N–H-stretching modes. The latter are generally broad bands and do therefore not hinder intensity measurements. Phosphatidylcholine however has a weak absorption band at 3025 cm^{-1} which is of similar band width. In order to estimate the mean direction of the $\text{C}=\text{C}$ double bond in egg phosphatidylcholine, Fig. 10, the dichroic ratios of $\nu(\text{C}=\text{C})$ and $\nu_{\text{as}}(\text{CH}=\text{CH})$ were determined to be $R_{\text{ATR}}(1610\text{ cm}^{-1})=1.17\pm 0.03$ and $R_{\text{ATR}}(3008\text{ cm}^{-1})=1.35\pm 0.05$. Finally it should be mentioned that the $\nu(\text{C}=\text{C})$ band is weakly structured. This may result from double bonds being located at different positions along the hydrocarbon chain. $\nu_{\text{as}}(\text{CH}=\text{CH})$ seems therefore to be more adequate for mean order parameter determination than

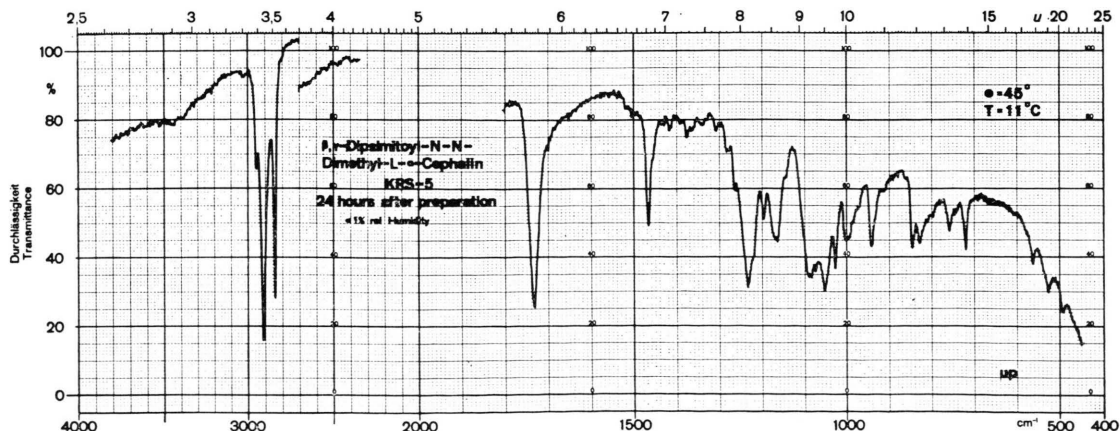


Fig. 8. Oriented layer of β, γ -dipalmitoyl-N,N-dimethyl-L- α -phosphatidylethanolamine (DPPDME) on a KRS-5 ATR plate. Recrystallized after 24 hours. up: unpolarized, $\vartheta=45^\circ$, $T=11^\circ\text{C}$, rel. humidity <1%.

$\nu(C=C)$. Furthermore in hydrated or protein doped samples the latter will be strongly overlapped by water and amide group vibrations, respectively.

The angle Θ has to be known to determine the order parameter by means of Eqn (3). In case of $\nu_{as}(CH=CH)$, Θ denotes the mean deviation of the double bond directions from the z -axis. If tentatively Θ is set zero the order parameter S' related to Eqn (6) is found to be $S' = 0.36 \pm 0.03$. However, $\Theta = 0$ must also be consistent with the dichroic ratios from other group vibrations, such as $\nu_s(CH_2)$ at 2845 cm^{-1} , $\nu_{as}(CH_2)$ at 2920 cm^{-1} , $\delta(\alpha\text{-CH}_2)$ at 1415 cm^{-1} and $\delta_s(CH_3)$ at 1375 cm^{-1} . R_z^{ATR} ($\nu_{as}(CH_2)$) as determined from band shape analysis is 1.13 ± 0.05 . The corresponding symmetric stretching vibration resulted in R_z^{ATR} ($\nu_s(CH_2)$) = 1.13 ± 0.1 . These values are contradictory to $\Theta = 0$ assuming that the mean direction

of the unsaturated hydrocarbon chain is parallel to the z -axis. If this would be the case the corresponding dichroic ratio should be expected to be $(E_x/E_y)^2 = 0.789 \leq R_z^{ATR} \leq (E_x/E_y)^2 + (E_z/E_y)^2 = 0.998$. The only explanation available at present from IR spectroscopy is that the hydrocarbon chains must be tilted in analogy to the findings with other phospholipids containing saturated hydrocarbon chains, *cf.* Table I. Thus if the same tilt angle is assumed for egg PC as for DPPC the resulting order parameter of the mean double bond direction may be estimated to be $S' = 0.60 \pm 0.10$. This result is consistent with recent NMR data from Seelig and Seelig³⁶ and Stockton *et al.*³⁷. The relatively large error of S' results predominantly from the uncertainty of the angle Θ . However, if on the other hand corresponding S' values are available, *e.g.* from NMR spectroscopy, then it will be possible

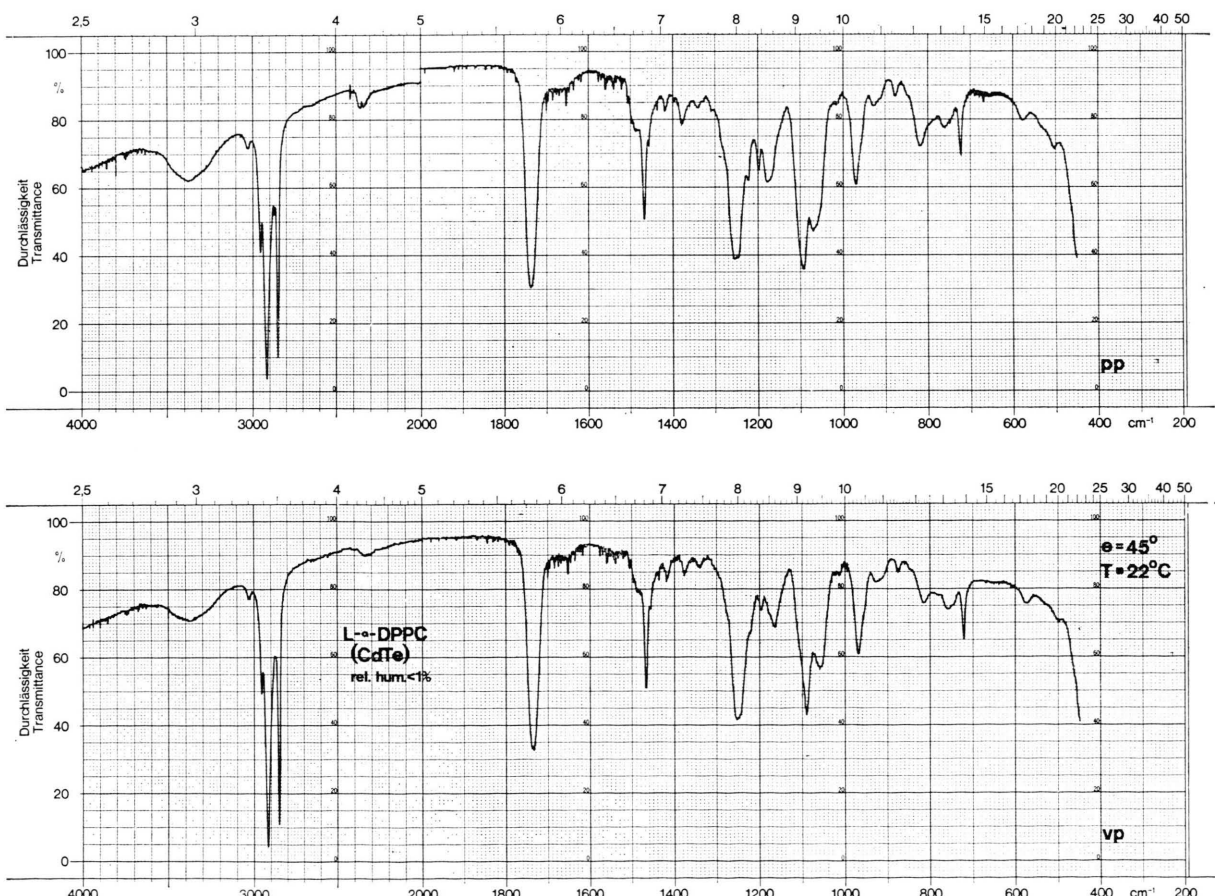


Fig. 9. Oriented layers of β,γ -dipalmitoyl- α -phosphatidylcholine (DPPC) on a CdTe ATR-plate. pp: parallel polarized, vp: perpendicular polarized, $\vartheta = 45^\circ$, $T = 11^\circ\text{C}$.

to determine the angle Θ from R_z^{ATR} with higher accuracy. Fig. 11 shows the Kratky distribution function and its integral for the direction of the double bonds of egg phosphatidylcholine. Since the transition dipole moments of $\delta(\alpha\text{-CH}_2)$ ($R_z^{\text{ATR}} = 0.88 \pm 0.05$), $\nu_s(\text{CH}_2)$, $\nu_{\text{as}}(\text{CH}_2)$ and $\delta_s(\text{CH}_3)$ deviate from the mean direction of the hydrocarbon chain the interpretation of Θ -value determined by means of the corresponding order parameter and Eqn (3) becomes more complicated than for transition moments directing along the hydrocarbon chain. However, it is obvious that relevant information with respect to molecular structure and orientation may be obtained via these off-axis transition moments. *E. g.* in order to explain the high values of the dichroic ratios of $\nu_s(\text{CH}_2)$ and $\nu_{\text{as}}(\text{CH}_2)$ (see above) it has been assumed that due to *gauche* defects the resulting transition moments are randomly

oriented in a plane perpendicular to the chain direction. This model, however, turned out to be inadequate since the calculated dichroic ratios were too small. Thus, chain ordering must be considerably higher.

4.3. The structure of polar headgroups

4.3.1. Structure of fatty acid ester groups

The vibrations of ester groups of fatty acids have been discussed earlier by many authors. The reader is referred to ref.³⁸⁻⁴⁰. The C=O double bond stretching vibration is known to be a good normal mode, its oscillating dipole moment can be assumed to lie parallel to the double bond. This enables an accurate determination of the double bond direction by means of polarization measurements. Two absorption bands are expected to occur correspond-

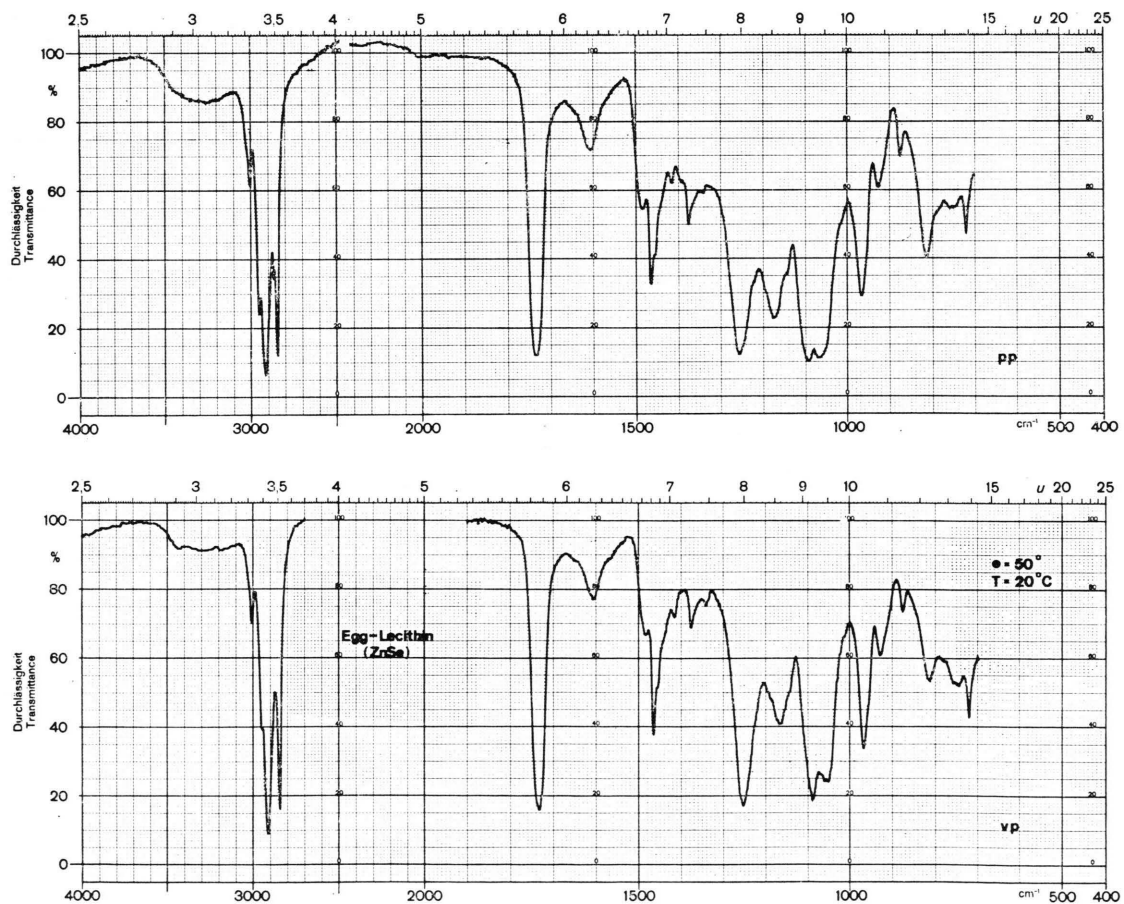


Fig. 10. Oriented layers of egg phosphatidylcholine (egg-PC) on a ZnSe ATR-plate. pp: parallel polarized, vp: perpendicular, polarized, $\vartheta = 50^\circ$, $T = 20^\circ\text{C}$.

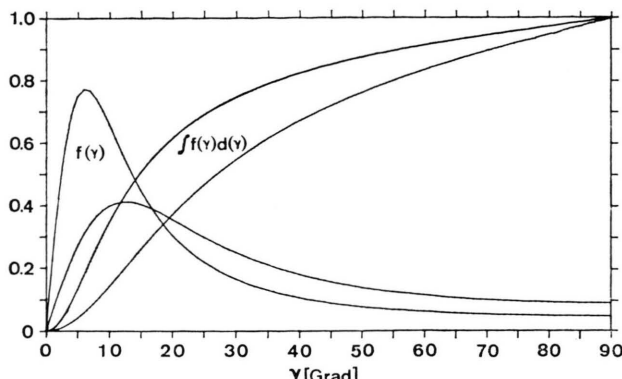


Fig. 11. Kratky distribution function $f(\gamma)$, Eqn (8), for the average direction of the double bonds in the unsaturated hydrocarbon chain of egg phosphatidylcholine (egg-PC).

$\int_0^\gamma f(\gamma) d\gamma$ denotes the averaged fractional number of double bonds pointing into the spherical sector $\Theta \pm \gamma$, ($\Theta \sim 31^\circ$ mean deviation of the unsaturated hydrocarbon chain from the normal to the bilayer, *cf.* Sec. 4.2.) Corresponding upper and lower curves indicate the limits of experimental error, which should be related to the order parameter $S' = 0.60 \pm 0.10$.

ing to the two carbonyl groups of the fatty acid esters. However, a significant band separation is observed only in the DPPE samples Figs 3 and 4. Obviously the band contour of $\nu(C=O)$ is very complex especially for DPPE oriented layers on germanium (Fig. 4). Bandshape analysis showed that the minimum number of Lorentzian bands²⁴ required for a approximate reproduction of this shape is 6. Position, halfwidth and areas of these components are shown in Table III. It should be noted that the two main components of DPPE on KRS-5 (Fig. 3) are seen as shoulders in the $\nu(C=O)$ band complex of DPPE on Ge (Fig. 4) and *vice versa* (*cf.* Table III). The complex line shapes observed with DPPE could result from different types of hydrogen bonds between the amino group of ethanolamine and the ester carbonyl groups. The strong shift of the $\nu(C=O)$ band to longer wavelengths in the sample prepared on germanium points to strong external hydrogen bonds⁵³. Therefore one should expect at least in this sample the polar headgroup of DPPE to assume several different conformations. As soon as the amine group is methylated (Figs 5–10) the distinct separation of $\nu(C=O)$ bands is lost. Although the band shape seems to be less complex now, it turned out that it cannot be reproduced either by a single (lysolecithin) by two (DPPE-DPPC) Lorentzian line shapes

because of band skewing at longer wavelength. There are probably two reasons for the distortion of the symmetric line shape, namely hydrogen bonding to water molecules and overlapping with the H_2O -bending ($\delta(H_2O)$) vibration¹⁴. This interpretation is supported by the observation that the shape of the $\nu(C=O)$ band becomes more symmetric when the sample is dried for several hours at $\sim 90^\circ C$ in a nitrogen atmosphere. At the same time the absorption bands of bound water are significantly reduced at $\sim 3400 \text{ cm}^{-1}$ ($\nu(H_2O)$) and at 1650 cm^{-1} ($\delta(H_2O)$).

In the case of lysolecithin there are at least 4 Lorentz bands required in order to get a reasonable fit of the $\nu(C=O)$ band in the $1800 - 1700 \text{ cm}^{-1}$ region (to be published). The results of this analysis are depicted in Table III. There is of course no stringent reason for the choice of the position and the half-width of the Lorentz band components. The main attention was paid to get a reasonable fit with a minimum number of Lorentz bands. Nevertheless his analysis had led to the interesting observation that the components are inhomogeneously polarized (Table III). This effect could result from ester groups with different conformations so that the $C=O$ double bonds point in different directions. However, in view of the findings with the $C-O$ single bond stretching vibration $\nu(C-O)$ at $1160 - 1180 \text{ cm}^{-1}$ (see below) one should rather expect the deviations of the $\nu(C=O)$ transition dipole moments to be induced by different types of hydrogen bonds to the carbonyl group. Unfortunately the conclusion must be drawn that it will be difficult to get reliable structural information via dichroic ratio measurements of the $\nu(C=O)$ band. As demonstrated by Table III the same arguments also hold for DPPC. In view of these findings the calculated directions of the oscillating dipole moments reported in Table III have to be considered as tentative results. Finally it should be mentioned that in case of DPPC the long wavelength tailing of the $\nu(C=O)$ band is found to be significantly smaller than in lysolecithin indicating most probably a different arrangement of the hydrogen bonds to the corresponding carbonyl groups. This observation is supported by hydration modulation measurements with oriented layers of DPPC and lysolecithin which showed that the hydration affinity of the carbonyl group of lysolecithin is considerably higher than that of the corresponding groups in

Table III. Characterization of $>\text{C}=\text{O}$ double bond stretching vibrations.

Substance ^a	Parameters of bandshape analysis			$R_{\text{ATR}} = \frac{A_{ }}{A_{\perp}}$ ^b	ϕ ^c	Comments ^d	
	ν_0	$\Delta\nu_{\frac{1}{2}}$	$A_{ }$				
DPPE	1753	4	2.10	1.11	1.88	58°	Fig. 4
	1750	3	1.32	1.56	0.85	0°	
	1743.5	2.6	1.60	1.36	1.18	39°	
	1738	4.8	8.21	6.87	1.19	40°	
	1733	3	7.15	4.68	1.53	52°	
	1722	8	40.85	23.21	1.76	56°	
DPPE (recryst.)	1753	4	1.57	2.08	0.76	0°	Fig. 3
	1750	3	—	—	—	—	
	1743.5	2.6	11.72	10.96	1.07	40°	
	1738	4.8	26.96	16.88	1.60	54°	
	1733	3	5.01	3.42	1.46	52°	
	1722	8	4.69	2.68	1.75	57°	
DPPC	1703	12	7.60	6.45	1.18	44°	Fig. 9
	1752	4	2.14	1.62	1.32	49°	
	1744	4	4.25	3.30	1.29	48°	
	1738	6	14.00	10.02	1.40	51°	
	1730	8	28.79	30.76	0.94	31°	
	1722	6	2.85	2.28	1.25	47°	
Egg-PC	1752	4	2.07	1.25	1.65	55°	Fig. 10
	1744	4	6.68	4.88	1.37	50°	
	1738	6	9.68	7.85	1.23	46°	
	1730	8	31.14	30.73	1.01	36°	
	1722	6	4.62	1.11	4.18	71°	
Lyso-PC	1744	4	3.00	2.62	1.15	38°	Ge-ATR-plate $\vartheta=45^\circ$, $T=21^\circ\text{C}$ rel. humidity $\sim 15\%$
	1738	6	10.71	8.93	1.20	40°	
	1730	8	26.16	26.60	0.98	20°	
	1720	12	13.68	8.30	1.65	54°	

^a For explanation of the abbreviations *cf.* Sec. 1.^b ATR dichroic ratio, *cf.* Eqn (3).^c Angle between the transition moment of $\nu(\text{C}=\text{O})$ and the plane of the bilayer, *cf.* Fig. 2.^d For further comments *cf.* Sec. 4.3.1.^e $A_{||}$ and A_{\perp} are the relative areas of the corresponding Lorentzian bands for parallel (||) and perpendicular (\perp) polarized light, respectively. The error of a band area is estimated to be $<5\%$.

DPPC ⁴¹. Furthermore it was found that the polar head group of lysolecithin shows significant conformational differences with respect to DPPC (to be published).

Besides the well known $\text{C}=\text{O}$ double bond stretching vibration $\nu(\text{C}=\text{O})$ which has been discussed above, several absorption bands are reported with $\text{C}-\text{O}$ single bond stretching involved. The most intensive one is in the region $1160-1180\text{ cm}^{-1}$ ⁴⁰. Jones ³⁹ assigned this band to a group



vibration of $-\text{CH}_2-\text{C}-\text{O}-\text{CH}_2-$. In oriented multilayers of tripalmitin, position and half width of this band were found to depend significantly on the conformation of the ester group. If the



$\text{C}-\text{C}-\text{O}-\text{C}$ moiety is planar, *i.e.* in the crystalline state of tripalmitin, the corresponding band ap-

pears at 1180 cm^{-1} . A deviation from this conformation shifts the band to lower wavenumbers. In molten tripalmitin the band appears near 1160 cm^{-1} . The opposite band shift was observed in the rearrangement process of tripalmitin Langmuir-Blodgett layers ¹¹.

Furthermore, distinct z -polarization is observed when the ester group is planar and the direction of hydrocarbon chains is approximately parallel to the z -axis. The 1180 cm^{-1} band has been assigned to the first band of this progression ^{7, 8} because of its similarity with bands of the wagging progression. In view of the results presented in Fig. 12 one may conclude that if there is a $\gamma_w(\text{CH}_2)$ band at 1180 cm^{-1} at all, it must have minor intensity compared with the ester band occurring at the same wavelength. Further arguments support this interpretation. Egg phosphatidylcholine does not exhibit a wagging sequence since the hydrocarbon chains

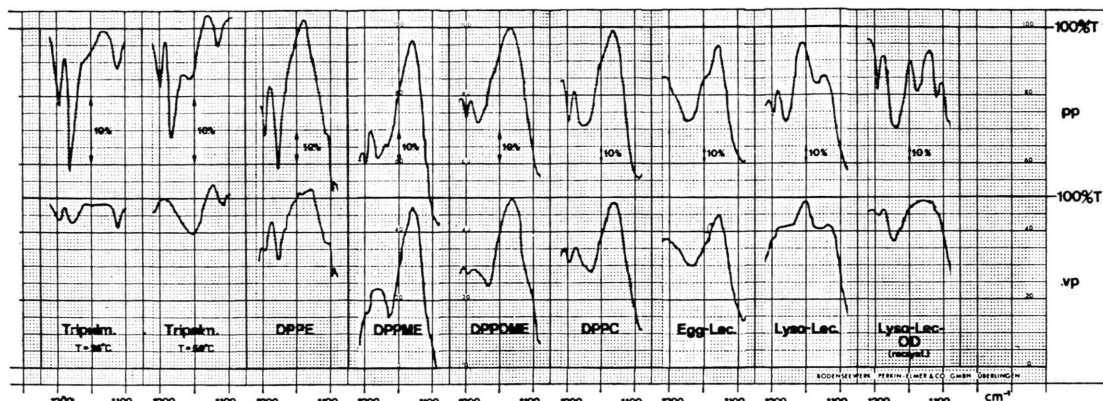


Fig. 12. C—O single bond stretching region of several fatty acid glycerol esters. Tripalm: tripalmitin, DPPE: dipalmitoylphosphatidylethanolamine, DPPME: dipalmitoylphosphatidyl-N-methylethanolamine, DPPDME: dipalmitoylphosphatidyl-N,N-dimethylethanolamine, DPPC: dipalmitoylphosphatidylcholine, EGG-lec: egg phosphatidylcholine, Lyso-lec: palmitoyl-lyso-phosphatidylcholine, Lyso-lec-O-D: O-deuterated palmitoyl-lyso-phosphatidylcholine (recrystallized). pp: parallel polarized, vp: perpendicular polarized. The 1180 cm^{-1} component indicates planar arrangement of the $\text{C}=\text{C}-\text{O}-\text{C}$ fragment, the non-planar conformation absorbs in the 1160 cm^{-1} region.

do not assume *all-trans* conformation at ambient temperature. Nevertheless a significantly polarized absorption band is observed near 1180 cm^{-1} (Fig. 12). The second example is lysolecithin in the crystallized and non-crystallized state. The latter exhibits a strongly polarized band at 1180 cm^{-1} which is shifted to 1170 cm^{-1} and partially depolarized upon recrystallization (Fig. 12). No $\gamma_w(\text{CH}_2)$ band appeared at 1180 cm^{-1} . Furthermore the polarizations of the $\gamma_w(\text{CH}_2)$ -progression and the shifted ester band are now significantly different. With respect to the conformation of the ester groups in the homologous series DPPE to DPPC it follows from polarization measurements that the ester band consists of two components whereas lysolecithin shows only one single band which corresponds to the high wavenumber component of the other phospholipids (Fig. 12). If the ester moiety leaves the planar conformation the 1180 cm^{-1} band is shifted to the 1160 cm^{-1} region. No corresponding low frequency component is observed at ambient temperature in the case of γ -L-palmitoyl-lyso- α -phosphatidylcholine (lysolecithin).

Thus, the following conclusions seem to be justified:

- The fatty acid ester group in γ -position exhibits planar configuration of the $\text{C}=\text{C}-\text{O}-\text{C}$ frame. The corresponding absorption band is near

1180 cm^{-1} and the oscillating dipole moment directs along the hydrocarbon chain.

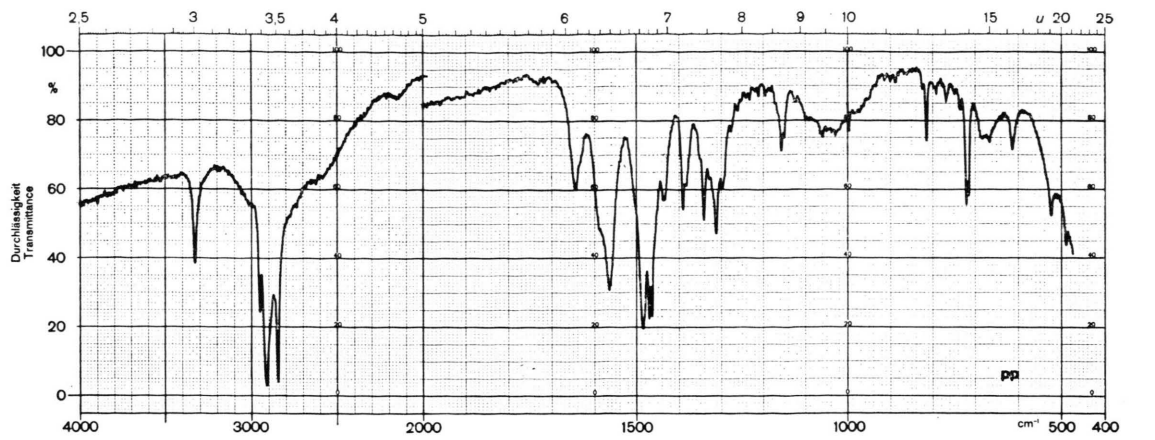
(ii) The fatty acid ester group in β -position of glycerol has no planar arrangement of the

$\text{C}=\text{C}-\text{O}-\text{C}$ fragment, which leads to a band shift from 1180 to 1165 cm^{-1} and to a considerable loss of polarization due to the conformational change.

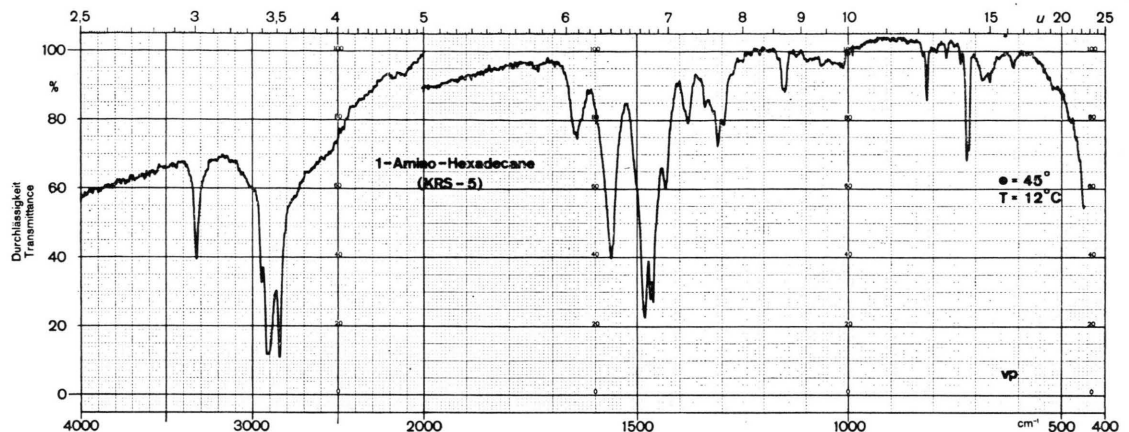
Our finding is in agreement with x-ray and NMR data published recently^{42–44} concerning DPPE.

4.3.2. Structure of the phosphate group

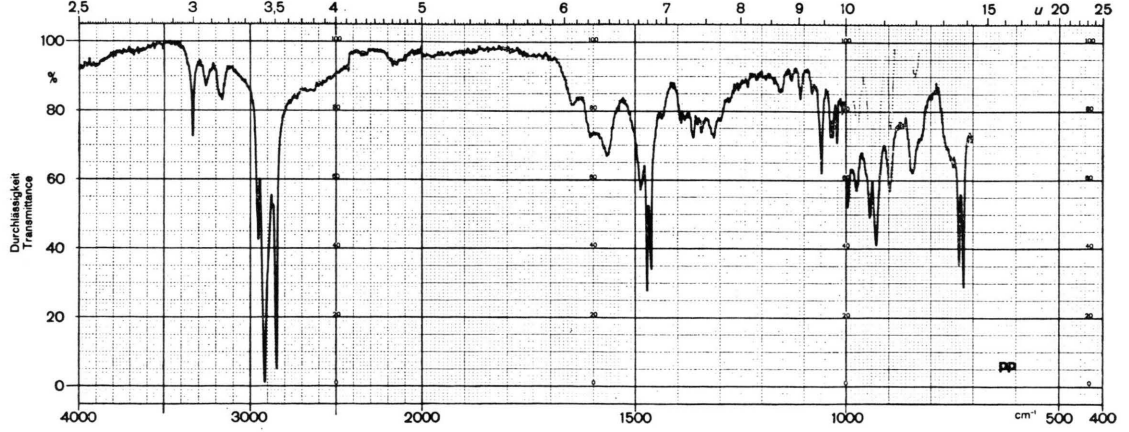
The polarizations of typical phosphate group vibrations, such as $\nu_{as}(\text{PO}_2^-)$ at $\sim 1230\text{ cm}^{-1}$, $\nu_s(\text{PO}_2^-)$ at $\sim 1090\text{ cm}^{-1}$, $\nu_{as}(\text{P}(\text{OR})_2)$ at $\sim 820\text{ cm}^{-1}$ and $\nu_s(\text{P}(\text{OR})_2)$ at $\sim 760\text{ cm}^{-1}$, is another common feature of the phospholipids under discussion (cf. Figs 3–10). Based on NCA results⁴⁵ the conformation of $\text{C}=\text{O}-\text{P}=\text{O}-\text{C}$ is assumed to be g^+/g^+ or g^-/g^- , respectively. $\nu_{as}(\text{PO}_2^-)$ at 1230 cm^{-1} exhibits no distinct polarization whereas the corresponding symmetric vibration $\nu_s(\text{PO}_2^-)$ at 1090 cm^{-1} shows typical parallel polarization. This observation leads to the conclusion that the angle between the bisector of $\text{O}-\text{P}-\text{O}$ of PO_2^- and the z -axis is smaller than 45° . This finding is in agreement with recent x-ray data of DPPE by Hitchcock *et al.*^{42, 43}, however, it is in contraction



(a)



(b)



(c)

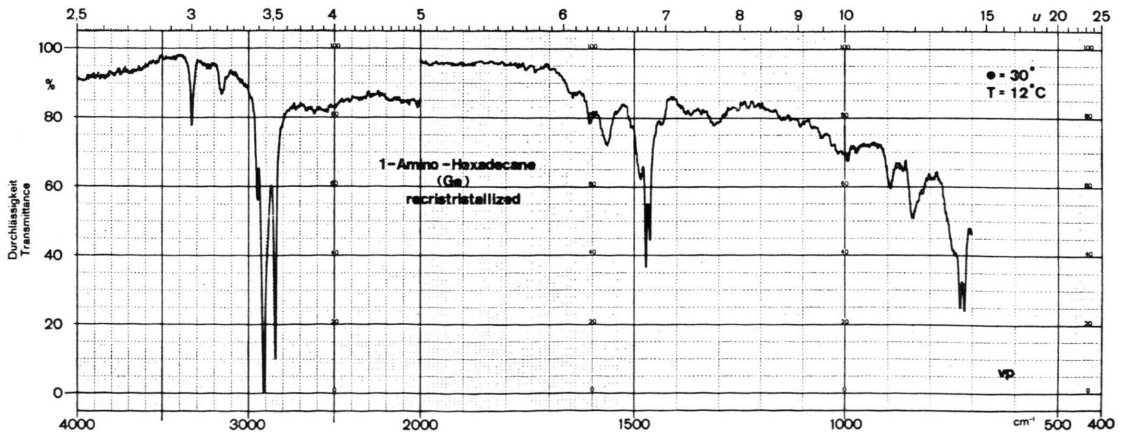


Fig. 13. Oriented layers of 1-aminohexadecane on a KRS-5 (a) and Ge (b) ATR-plate. pp: parallel polarized, vp: perpendicular polarized, $\vartheta = 30^\circ$ (a) and 45° (b), $T = 12^\circ\text{C}$.

with *x*-ray results from Phillips *et al.*⁴⁶ as well as with recent NMR investigations by Hauser *et al.*⁴⁷.

The authors conclude that the polar group in DPPC is extended and normal to the plane of the bilayer⁴⁶. It should be noted, however, that this result is obtained through a extrapolation procedure which necessarily must lead to a considerable loss of accuracy. In reference 47 DPPC bilayer vesicles have been investigated using paramagnetic probes. This system however is significantly different from the oriented phospholipid layers used in this work.

The assignment of PO-single bond stretching vibrations $\nu_{as}(P(OR)_2)$ at $\sim 820 \text{ cm}^{-1}$ and $\nu_s(P(OR)_2)$ at $\sim 760 \text{ cm}^{-1}$ ⁴⁵ is supported by a weak polarization of the 760 cm^{-1} band in the Raman spectrum¹⁸. In order to explain our polarization measurements one has to assume that $\nu(C-O)$ of the $C-O-P-O-C$ fragment is significantly involved in these vibrations.

4.3.3. Structure of ethanolamine group

Recently Akutsu *et al.* have published infrared transmission studies of phosphatidylethanolamine from *E. coli* and dipalmitoyl phosphatidylethanolamine (DPPE)^{7,8}. Earlier IR-investigations of DPPE and a number of other phospholipids have been carried out by Abramson *et al.*⁵. These authors concluded that in CCl_4 -solution the phosphate group of phosphatidylethanolamine and phosphatidylserine is in the protonated state,

$\text{O}=\text{P}-\text{OH}$, whereas lecithin and sphingomyelin have ionized phosphate groups, $>\text{PO}_2^-$. This finding is in contradiction to that of Akutsu *et al.*^{7,8} who postulated the ionized form, *i.e.* the existence of the $>\text{PO}_2^-$ and $-\text{NH}_3^+$ groups, respectively. In view of our findings the interpretation given by Abramson *et al.*⁵ seems to be more reasonable

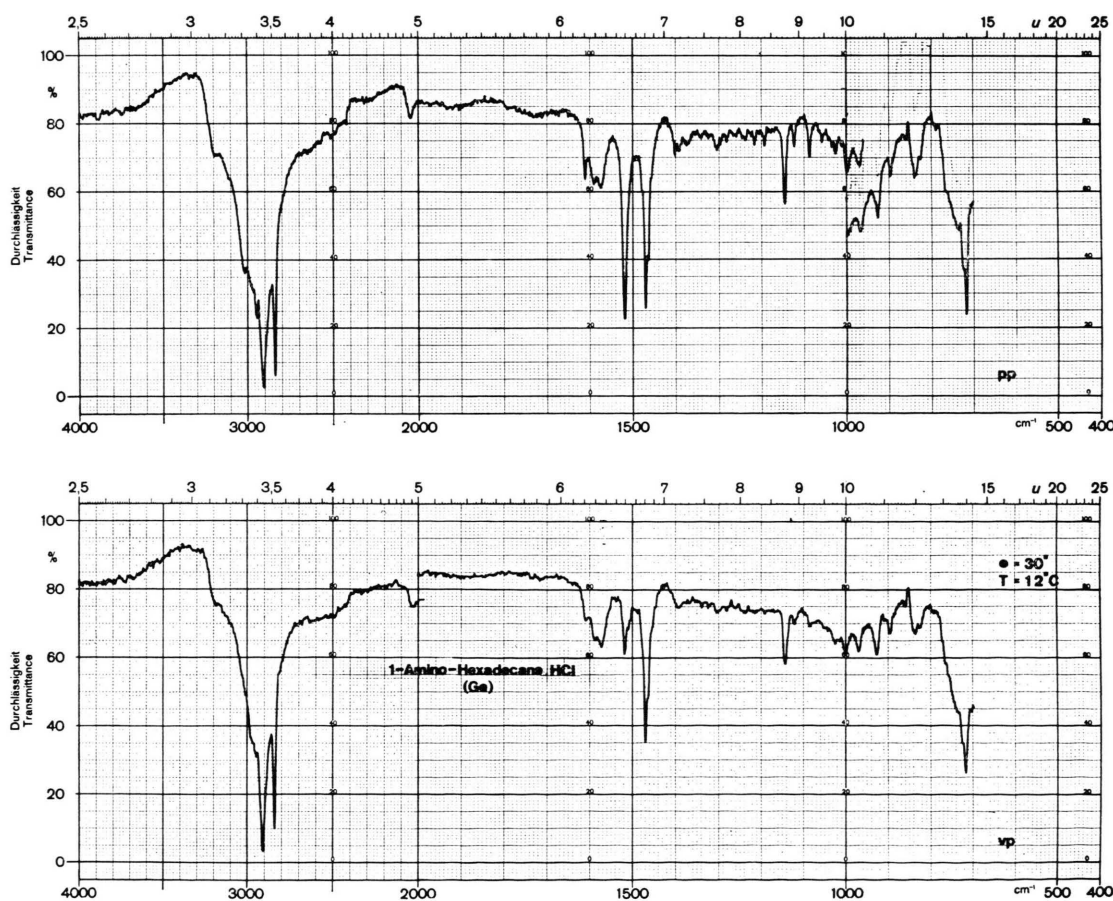


Fig. 14. Oriented layers of 1-aminohexadecane·HCl on a germanium ATR-plate. Sample of Fig. 13 a after exposure to HCl gas. pp: parallel polarized, vp: perpendicular polarized, $\vartheta=30^\circ$, $T=12^\circ\text{C}$.

especially so for the crystalline state. Although no definite interpretation can be given at present, some features of DPPE as derived from Figs 3–5 are summarized below.

(a) Facts pointing to a protonated phosphate group:

Oriented layers of 1-amino-hexadecane (Fig. 13 a) show strong absorption bands at 1482, 1560, 1590 and 1645 cm^{-1} . Exposures to HCl gas results in the hydrochloride of the amine (Fig. 14). The corresponding absorption bands are observed at 1520, 1572, 1590 and 1610 cm^{-1} . Furthermore a new band appears at 2045 cm^{-1} . The bands below 2000 cm^{-1} have to be ascribed to deformation vibrations of the $-\text{NH}_2$ and $-\text{NH}_3^+$ groups, respectively. The 2045 cm^{-1} band is typical for the $\text{C}-\text{NH}_3^+$ group^{48, 49}. In the spectrum of DPPE oriented

layers neither the 1520 cm^{-1} nor the 2045 cm^{-1} bands are observed. It should be mentioned that the 2130 cm^{-1} band exists also in the spectrum 1-amino-hexadecane (Fig. 13 a, b). Corbridge⁵⁰ has investigated a great number of phosphate compounds. He found that the $-\text{P}-\text{OH}$ group gives rise to a medium or strong absorption band in the 1200–1400 cm^{-1} region. He proposed a correlation with a POH deformation mode. A corresponding strong and polarized absorption band is observed at 1256 cm^{-1} in the case of the PE-analogue, *i.e.* the fatty acid ester groups replaced by a ketal group, Fig. 15. This band was absent in noncrystallized PE-analogue samples. Simultaneously the 1560 cm^{-1} band was shifted to 1530 cm^{-1} , where $\delta_s(-\text{NH}_3^+)$ is expected. In DPPE (Figs 3, 4) the absorption band corresponding to the 1256 cm^{-1}

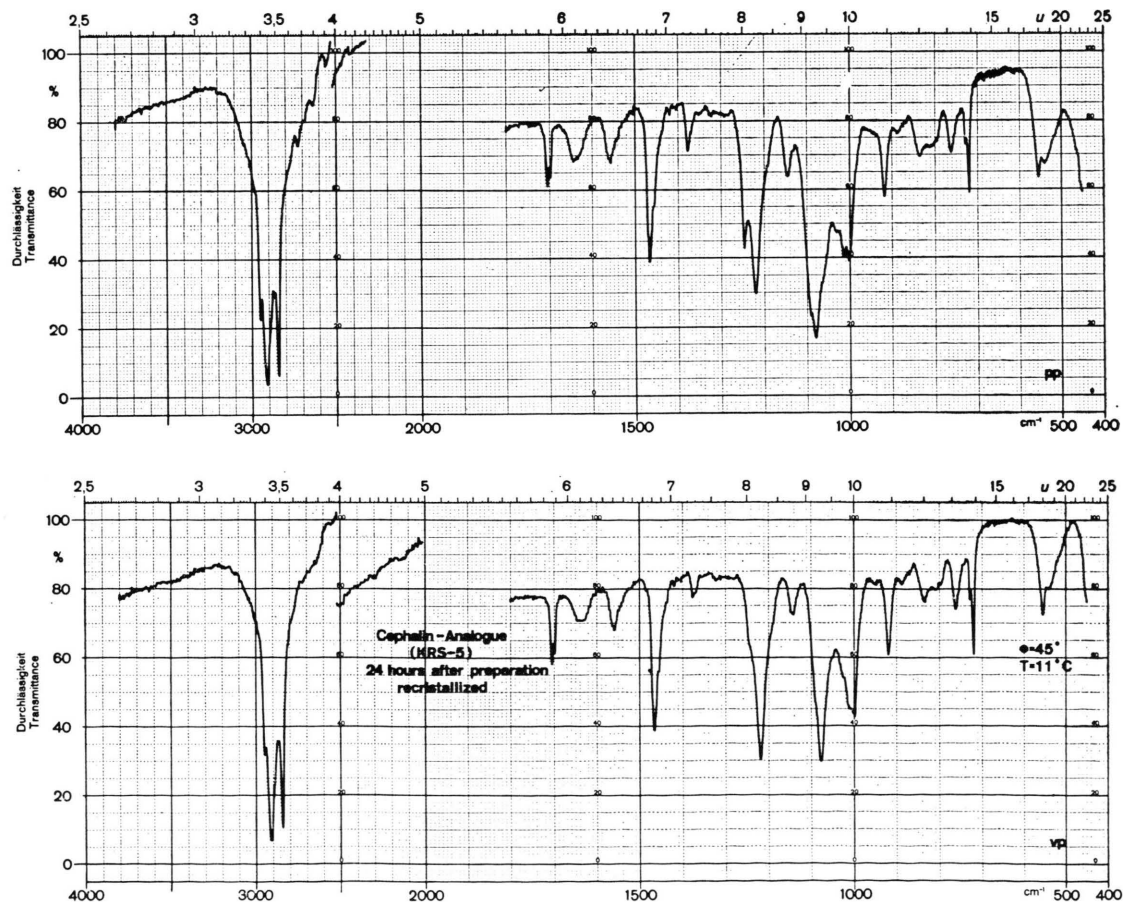


Fig. 15. Oriented layers of ketal phosphatidylethanolamine (PE-analogue) on a KRS-5 ATR-plate. Recrystallized. pp: parallel polarized, vp: perpendicular polarized, $\vartheta=45^\circ$, $T=11^\circ\text{C}$.

band ($\delta(\text{POH})$) of the PE-analogue could not be identified which may be due to overlapping with a $\gamma_w(\text{CH}_2)$ band. Natural phosphatidylethanolamine from sheep brain (sh. br. PE) results in a significantly different infrared spectrum (Fig. 5) compared with DPPE (Figs 3, 4). The principal differences are:

(i) No crystallinity, broad and overlapping bands.

(ii) The polar part of natural DPPE binds water under conditions where synthetic DPPE does not. This fact may be one reason for the band broadening of $\nu(\text{C=O})$ and $\nu(\text{PO}_2^-)$ due to hydrogen bonding with adsorbed water.

(iii) The N—H-deformation mode in the 1500—1600 cm^{-1} region appears at 1535 cm^{-1} thus pointing to the existence of the NH_3^+ -group (cf. 1-aminohexadecane·HCl, Fig. 14).

(iv) The intense absorption band observed at 1015 cm^{-1} in DPPE (Figs 3, 4) is not observed in sheep brain cephalin thus indicating that the structure of the polar headgroup is altered. Akutsu *et al.*^{7, 8} have assigned this band to $\nu_{\text{as}}(\text{CCN})$. Furthermore, they found this band to be very sensitive to N-deuteration. Assignment and observation are in agreement with a normal coordinate analysis of gaseous methylamine by Dellepiane and Zerbi⁵¹, who have assigned the 1044 cm^{-1} band to the undisturbed C—N stretching mode. Deuteration shifts this band to 997 cm^{-1} due to alteration of the normal mode. After deuteration, however, only 80% of the potential energy may be ascribed to CN stretching and 20% to ND_2 deformation. In view of these observations one would expect that the 1015 cm^{-1} mode should also be sensitive to protonation of the amino group.

(b) Direction of hydrocarbon chains with respect to the plane of bilayers

The plane of bilayers is assumed to lie parallel to the xy -plane of the ATR-plate (Fig. 1). Concerning the direction of the hydrocarbon chains the reader is referred to Sect. 4.2. and to Table I.

(a) Orientation of the phosphate group

$\nu_{\text{as}}(\text{PO}_2^-)$:

In case of DPPE this band probably originates from $\nu(\text{P=O})$ of the $>\text{PO}_2\text{H}$ group. It overlaps with the $\gamma_w(\text{CH}_2)$ progression. No accurate deter-

mination of the dichroic ratio is possible unless line shape analysis is performed. However, since no distinct zz -polarization is observed this transition moment may be estimated to be more or less parallel to the plane of bilayers, in agreement with Akutsu's findings⁸.

$\nu_s(\text{PO}_2^-)$:

This absorption band is expected in the 1090—1100 cm^{-1} region (cf. Sec. 3.2.). Most phospholipids show a distinct zz -polarization (Figs 5—10) thus indicating that the bisector of $\angle(\text{OPO})$ directs towards the z -axis. However, this behaviour is neither clearly found in crystalline DPPE (Figs 3, 4) nor in the corresponding ketal compound (Fig. 15). Concerning the latter it should be mentioned that the strong absorption band at 1090 cm^{-1} probably results from a vibration of the ketal group⁵². For a detailed discussion of general features the reader is referred to Sec. 4.3.2.

(d) Conformation of $\text{O}-\text{C}-\text{C}-\text{N}$, $\text{P}-\text{O}-\text{C}-\text{C}$, $\text{P}-\text{O}-\text{C}_\alpha-\text{C}_\beta$ (glycerol) and $\text{O}_\beta-\text{C}_\beta-\text{C}_\gamma-\text{O}_\gamma$ (glycerol) moieties

No direct information is available so far from IR spectra. Akutsu *et al.*⁸ have proposed *gauche* conformation for $\text{O}-\text{C}-\text{C}-\text{N}$ and $\text{O}_\beta-\text{C}_\beta-\text{C}_\gamma-\text{O}_\gamma$ and *trans* conformation for $\text{P}-\text{O}-\text{C}_\alpha-\text{C}_\beta$ and $\text{P}-\text{O}-\text{C}-\text{C}$ (ethanolamine), however, available IR spectroscopic arguments are not sufficient to reliably support their picture.

(e) C=O double bond vibrations

In contrast to the other phospholipids under discussion *cf.* Sec. 4.3.1. two bands are clearly resolved in DPPE. The low frequency component at 1724 cm^{-1} is considerably broader (Fig. 4). This may be due to the different molecular environments of the two carbonyl groups in β - and γ -position, respectively. This conclusion was also drawn from the polarization behaviour of the fatty acid ester vibration in the 1160—1180 cm^{-1} region (Sec. 4.3.1.). Broadening of the 1724 cm^{-1} band may be due to hydrogen bonding to this group⁵³. The DPPE sample which was prepared on KRS-5 (Fig. 3) is of much better crystallinity. An interesting feature of this sample is its hydrophobicity. No differences could be detected in the infrared spectrum whether the sample was exposed to 0% or to 90% relative humidity at ambient temperature. This

hydrophobic behaviour could explain shifts of the $\nu(\text{C}=\text{O})$ band from the $1720 - 1730 \text{ cm}^{-1}$ region (Fig. 4) to the 1740 cm^{-1} region (Fig. 3). Significant changes with respect to the $>\text{C}=\text{O}$ orientation were found (*cf.* Table III), indicating that recrystallization must have occurred. This conclusion gets further support by the fact that the shapes of the complex $\nu(\text{C}=\text{O})$ bands of the DPPE samples (Figs 3, 4) could be approximated with the same set of Lorentz bands.

4.3.4. Special features of N-methyl-phosphatidyl-ethanolamine

The spectrum of DPPME is presented in Fig. 6. Concerning the structure of hydrocarbon chains, the ester groups and the phosphate groups, the reader is referred to Sections 4.2., 4.3.1. and 4.3.2. and Tables I, II. Little information is available about N-methylethanolamine, however extensive investigations of dimethylamine have been carried out by Dellepiane and Zerbi⁵¹ and Buttler and McKean⁵⁴. The latter have also reported crystal spectra. Recently Gamer and Wolff⁵⁵ have reported vibrational frequencies of gaseous secondary aliphatic amines obtained by means of infrared and Raman spectra. The characteristic features of the polar head group of DPPME are first its CNC-plane, which was found to be predominantly parallel to the xy -plane and secondly the phosphate group, which was found to be in the deprotonated state, *i.e.* $>\text{PO}_2^-$. The arguments leading to these conclusions are depicted below.

$\nu_{\text{as}}(\text{CNC})$: 1031 cm^{-1}

Based on normal coordinate treatment⁵¹ this vibration has to be considered as a combination of antisymmetric CN-stretching ($\nu_{\text{as}}(\text{CNC})$) and in plane methyl rocking ($\gamma_r(\text{CH}_3)$). The oscillating dipole moment may be assumed to be directed along the C–C interconnecting line. The polarization observed in Fig. 6 indicates that the corresponding C–C direction is approximately parallel to the xy -plane, ($R_z^{\text{ATR}} = 0.85 \pm 0.10$; $\Phi = 0^\circ - 30^\circ$).

$\nu_s(\text{CNC})$: 960 cm^{-1}

This vibration consists predominantly of symmetric CNC-stretching ($\nu_s(\text{CNC})$). Thus the resulting oscillating dipole moment should be directed along the bisector of the CNC angle. The cor-

responding dichroic ratio is found to be $R_z^{\text{ATR}} = 0.91 \pm 0.04$, *i.e.* $\Phi = 24^\circ - 32^\circ$. Φ denotes the angle between the transition dipole moment and the plane of the bilayer (xy -plane). One may suggest therefore that the CNC plane is predominantly parallel to the xy -plane.

Antisymmetric H-bending of N-methyl group $\delta_{\text{as}}(\text{N}-\text{CH}_3)$:

This band appears as a weak shoulder at $\sim 1500 \text{ cm}^{-1}$. In methyl amine compounds it is observed $20 - 40 \text{ cm}^{-1}$ lower^{51, 54, 55}. The shift to higher wavenumbers could be interpreted as induced by the positively charged ammonium group, since the same shift is also observed in the case of lecithin, choline, N-trimethyl-1-amino-hexadecan, tetramethylammonium etc. The 1500 cm^{-1} band shows no polarization thus confirming the postulate that the CNC plane is approximately parallel to the xy -plane. (Since the corresponding oscillating dipole moment (E-type mode, *cf.* ref.²²) is in the plain perpendicular to the $\text{N}-\text{CH}_3$ bond.)

NH-deformation

The phosphate group of DPPE is expected at first sight to be in the protonated state $>\text{PO}_2\text{H}$. However, from IR spectra of the N-monomethyl derivative one rather has to conclude it to be deprotonated (*i.e.* $>\text{PO}_2^-$) intramolecularly by the $-\text{NHCH}_3$ group. Arguments for this interpretation are based on the vibration bands of the phosphate group in the $1050 - 1100 \text{ cm}^{-1}$ range. In this region these bands show close similarity to those of lecithin. Furthermore in the spectra of DPPME an absorption band at 1630 cm^{-1} is observed which may be attributed to $\delta(\text{NH}_2)$ of the $\text{C}-\text{NH}_2\text{CH}_3^+$ group. In neutral $-\text{NHCH}_3$ group this band should be absent^{51, 54, 55}.

NH-stretching

$\nu(\text{NH})$ in secondary amines is observed in the 3300 cm^{-1} region^{51, 54, 55}. With DPPME there is no absorption band observed in the 3300 cm^{-1} region, however, two distinct bands appear at 2720 and 2490 cm^{-1} . A preliminary assignment is $\nu_{\text{as}}(>\text{NH}_2^+)$ and $\nu_s(>\text{NH}_2^+)$. These findings are supported by the IR-spectrum of ethylmethylamine hydrochloride (unpublished results).

4.3.5. Special features of N–N-dimethylphosphatidylethanolamine

CN-Stretching

Only a tentative assignment based on normal coordinate analysis of choline by Rihak *et al.*^{13, 56} is available so far. Two strong bands are observed in the 900–1000 cm^{−1} region. They are ascribed to the symmetric (945 cm^{−1}) and antisymmetric (995 cm^{−1}) N–CH₃ stretching vibrations, whereas the weak band at 1025 cm^{−1} could result from a O–C–C–N stretching mode with ν (C–O) and ν (C–N) in antiphase, resulting in an oscillating dipole moment directing approximately along the C–C– bond of the ethanolamine part. The oscillating dipole moments of ν_s (CN) at 945 cm^{−1} and ν_{as} (CN) at 995 cm^{−1} should be directed approximately along the bisector of CH₃–N–CH₃ and along the line connecting the two C atoms, respectively, *i.e.* approximately perpendicular to each other. The dichroic ratios as determined from Fig. 7 are R^{ATR} (995 cm^{−1}) = 1.17 ± 0.05 and R^{ATR} (945 cm^{−1}) = 0.85 ± 0.05. The mean angles between the transition moments and the *xy*-plane are found to be Φ (995 cm^{−1}) = 42°–46° and Φ (945 cm^{−1}) = 9°–27°. This indicates, that there exist one or at most two preferred conformations of the N–(CH₃)₂-group with respect to the C–C bridge of ethanolamine. Otherwise both absorption bands should exhibit a dichroic ratio of approximately R^{ATR}_{iso} = 1.00.

NH-deformation and NH-stretching

The 1630 cm^{−1} band observed in DPPME is lacking, obviously due to substitution of a H atom by a methyl group. The γ_r (NH) vibration which in sesondary amines is expected to occur near 1500 cm^{−1} could not be identified, however, the broad and weakly structured band between 2300–2700 cm^{−1} may be ascribed to (R₃)⁺N–H stretching. In phosphatidylcholine (see below) no band is observed in this region.

4.3.6. Special features of phosphatidylcholine (lecithin)

Relatively detailed information on the choline part of lecithin is available from IR-spectra via symmetry considerations with simple model compounds and via a normal coordinate analysis of choline by Rihak *et al.*^{13, 56}. Comparison of the IR-

spectra of crystalline N(CH₃)₄Cl, choline, acetylcholine, glycerophosphorylcholine and phosphatidylcholine leads to the conclusion that 3–4 common bands observed in the 850 to 1000 cm^{−1} region must originate in the R–N(CH₃)₃⁺ group. Edsall⁵⁷ on the other hand reported that N(CH₃)₄⁺ in aqueous solution results in only one single Raman line near 955 cm^{−1} which may be assigned to the threefold degenerate (F₂-type²²) C–N-stretching vibration (tetrahedral symmetry of N(CH₃)₄⁺ in aqueous solution). This band should split into three absorption bands when the symmetry is decreased to C_s or lower, which is indeed the case for crystalline N(CH₃)₄Cl⁵⁸. The resulting three absorption bands are observed at 915, 945 and 955 cm^{−1}. Corresponding triplets are observed in the spectra of CH₃–(CH₂)₁₄–N(CH₃)₃Cl, choline, acetylcholine, phosphorylcholine and phosphatidylcholine, respectively. However the band situated at ~920 cm^{−1} is in some cases shifted to ~890 cm^{−1}, which depends most probably on the conformation of O–C–C–N in the choline part⁵⁶. Based on symmetry considerations and on NCA results this band is assigned to the symmetric –N(CH₃)₃⁺ stretching. The resulting oscillating dipole directs along the local C₃-symmetry axis of –N(CH₃)₃⁺. This vibration turned out to be of considerable importance for structural studies of the headgroup. The doublet in the 960 cm^{−1} region (Figs 9, 10) may be assigned in the framework of this approximation to the symmetric and antisymmetric CN stretching vibration of the N(CH₃)₃ system, respectively. The corresponding oscillating dipole moments are expected to be in the plane and perpendicular to the plane symmetry.

The most usefull results with respect to structural analysis are summarized below:

(i) The symmetric –N–(CH₃)₃ stretching (ν_s (N–(CH₃)₃) in choline is found to depend strongly on the torsion angle of the C–C-bond. For the *trans* conformation the absorption band is calculated to be at ~930 cm^{−1}, whereas the *gauche* conformation results in a band at ~890 cm^{−1}. Wyckoff⁵⁸ concluded from x-ray data that the conformation is *gauche* in the crystalline state. Experimentally NCA calculations of ν_s (N–(CH₃)₃) are confirmed. When the choline sample was prepared on zinc selenide by evaporating the solvent (H₂O) the still strongly hydrated choline showed a band at 924 cm^{−1} in good agreement with the calculated

$\nu_s(N-(CH_3)_3)$ for the *trans* conformation. On drying, this band decreases while the 894 cm^{-1} band increases synchronously. This behaviour is typical for $\nu_s(N-(CH_3)_3)$ when the O—C—C—N frame assumes *gauche* conformation. There is no doubt that a direct relation between the two bands exists. *Trans-gauche* isomerisation is the only explanation available from NCA at present⁵⁶.

(ii) Another absorption band of diagnostic importance was calculated and observed in the 1020 cm^{-1} region. The oscillating dipole moment is estimated to lie parallel to the C—C bond of choline.

(iii) Concerning the doublet observed at $\sim 950\text{ cm}^{-1}$ NCA confirms the empirical assignment especially with respect to C_s -symmetry, *i.e.* *trans* or *cis* conformations.

(iv) The choline absorption band observed at 860 cm^{-1} was found to result from in-phase rocking $\gamma_r(CH_2)$ of the two methylene groups. This

motion is coupled with $\nu_{as}(N(CH_3)_3^+)$. The resulting oscillating dipole moment lies approximately in a plane normal to the C—C bond.

Application of these findings to the structure analysis of the polar headgroup of phosphatidylcholine leads to the following conclusions:

(i) Conformation of O—C—C—N fragment

Since the corresponding absorption bands are observed at $920-930$ and at 875 cm^{-1} , respectively, a mixture of probably *trans* and *gauche* isomers must also be expected in lecithin in analogy to the observation of at least two different isomers in hydrated choline⁵⁶. The 925 cm^{-1} band which is tentatively assigned to $\nu_s(N(CH_3)_3)$ of the *trans* conformation is considerably broader than the corresponding band in *gauche* conformation. No definite explanation of this fact can be

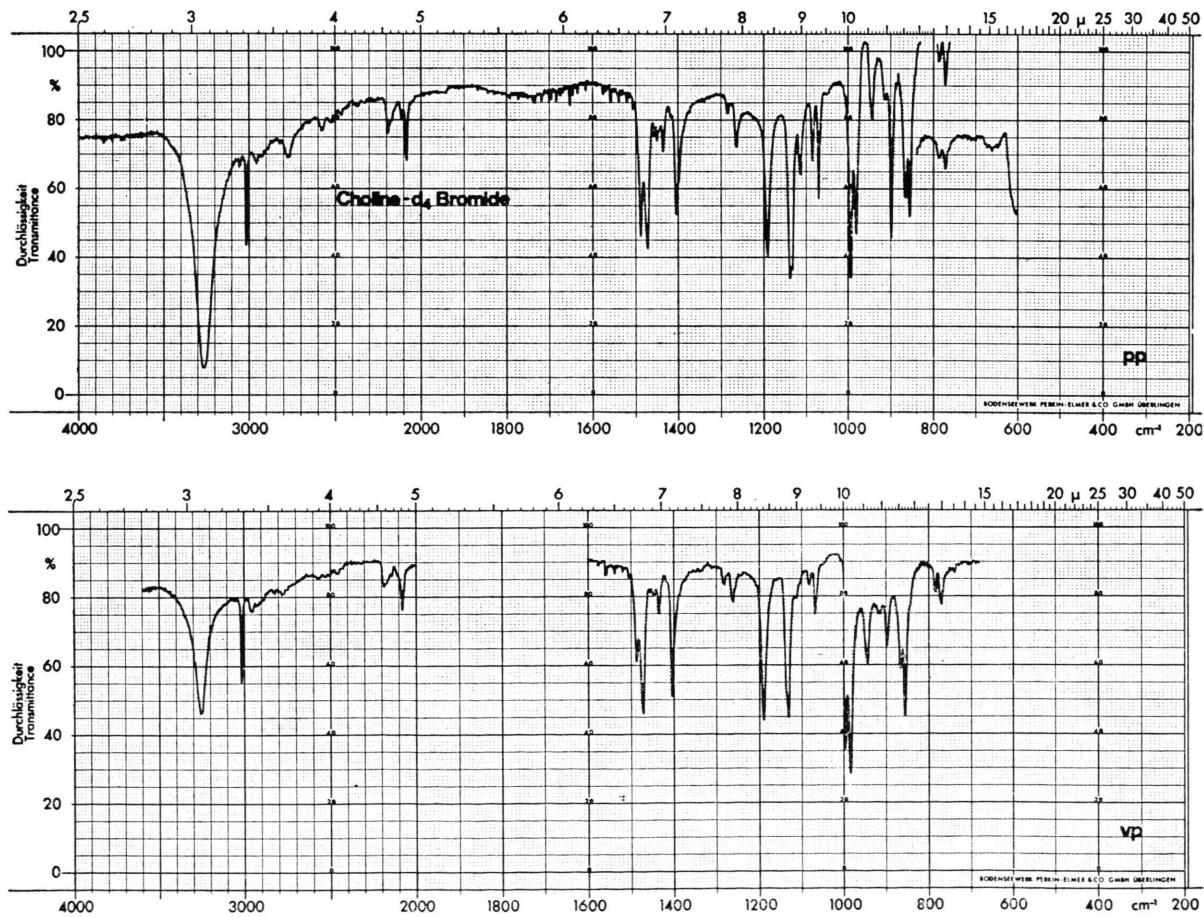


Fig. 16. Oriented microcrystals of choline-d₄ on a KRS-5 ATR-plate. $T=25\text{ }^\circ\text{C}$.

given at present, however, rotamers with respect to $-\text{N}(\text{CH}_3)_3$ and/or enhanced interaction with surrounding molecules could play a role. In the case of lysolecithin corresponding broadening of the 927 cm^{-1} band occurs to a smaller extent (to be published).

(ii) Direction of " C_3 "-symmetry axis of $-\text{N}(\text{CH}_3)_3$

(a) As mentioned above the transition dipole moment of $\nu_s(\text{N}(\text{CH}_3)_3)$ is estimated to be parallel to the local C_3 -symmetry axis. From the corresponding dichroic ratios $R_{\text{trans}}^{\text{ATR}}$ (925 cm^{-1}) = 1.00 ± 0.05 and $R_{\text{gauche}}^{\text{ATR}}$ (875 cm^{-1}) = 1.50 ± 0.02 one may determine the angular range between the C_3 -axis and the xy -plane. For MCU-type ultrastructure (Fig. 2) it is found to be $\varPhi^{\text{trans}} = 32^\circ - 39^\circ$, and $\varPhi^{\text{gauche}} = 52^\circ - 54^\circ$, respectively.

(b) Information about the mean direction of the C_3 -symmetry axis may be obtained via the bending modes of the N -methyl groups. Empirical assignment is based on the comparison of the ATR-IR spectra of methylene deuterated choline- d_4 (Fig. 16), methyl deuterated choline- d_9 and choline- d_0 . In the case of choline- d_4 at least four prominent CH_3 -bending modes are observed at $1488, 1472, 1405$ and 1400 cm^{-1} the highest and lowest bands being strongly polarized, *cf.* Fig. 16. Considering the $-\text{N}(\text{CH}_3)_3$ fragment as a subsystem with C_{3v} covering symmetry one expects the methyl bending fundamentals to be classified as $2\text{ A}_1 + \text{A}_2 + 3\text{ E}$ with the A_1 and E modes being IR active and polarized \parallel and \perp with respect to the local C_3 -axis, *i.e.* the direction of the $\text{C} - \text{N}(\text{CH}_3)_3$ bond. Though the molecule as a whole has at the most C_s symmetry the use of local C_{3v} symmetry

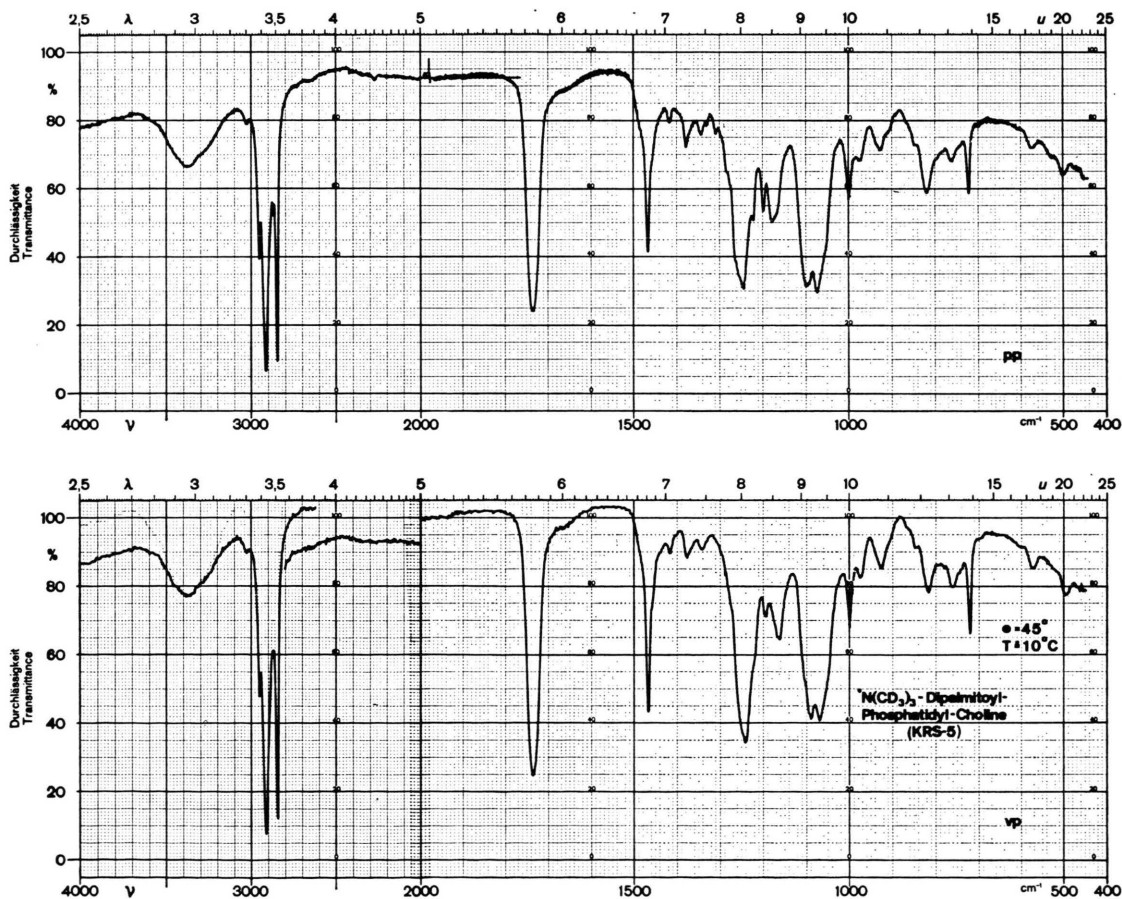


Fig. 17. Oriented layers of β,γ -dipalmitoyl- $\text{L}-\alpha$ -phosphatidylcholine- d_9 (DPPC- d_9) on a KRS-5 ATR-plate. pp: parallel polarized, vp: perpendicular polarized, $\vartheta = 45^\circ$, $T = 10^\circ\text{C}$.

for the methyl bending modes appears justified. One may therefore assign the 1488 and 1400 cm^{-1} bands as A_1 , the 1472 and 1405 cm^{-1} bands as E type modes. This is consistent with the assignment of polarized bands at 916 cm^{-1} (*trans*) and 898 cm^{-1} (*gauche*) as $\nu_s(\text{C} - \text{N}(\text{CH}_3)_3)$, since this mode should have the same oscillating dipole direction as the A_1 methyl bending modes. The arguments just presented form the basis for the use of the polarization of the 1488 cm^{-1} band as a diagnostic tool to derive of information about the average $\text{C} - \text{N}(\text{CH}_3)_3$ direction with respect to the coordinate system defined in Fig. 1. These arguments may be used to elucidate the conformation problem of the choline part of lecithin. It should be mentioned however that in phosphatidylcholine the $\delta_s(\text{N} - \text{CH}_3)$ doublet is shifted to the 1380 cm^{-1} region, thus overlapping with $\delta_s(\text{CH}_3)$ of hydrocarbon chains. In N-methyl deuterated phosphatidylcholine (Fig. 17) the doublet appears at 999 cm^{-1} and at 975 cm^{-1} , corresponding to the isotope shifts expected for $\text{H} \rightarrow \text{D}$ substitution. In the spectrum of DPPC-d₀ (Fig. 9) $\delta_{as}^{A_1}$ ($\text{N} - \text{CH}_3$) is found to be slightly z -polarized thus indicating that the mean direction of the C_3 -axis slightly deviates from the xy -plane. More detailed information about this direction is obtained via DPPC-d₉ (Fig. 17), since the corresponding $\delta_s^{A_1}$ ($\text{N} - \text{CD}_3$) band at 975 cm^{-1} is only weakly overlapped the corresponding E -type band at 999 cm^{-1} . The dichroic ratio is determined to $R^{ATR}(\delta_s^{A_1}(\text{N} - \text{CD}_3)) = 1.15 \pm 0.05$ pointing to a mean deviation of the C_3 -axis of $40^\circ - 46^\circ$ from the xy -plane (MCU-type).

Direction of the $\text{C} - \text{C}$ bond in the choline part

The weak band at 1014 cm^{-1} with dichroic ratio $R^{ATR} = 1.20 \pm 0.20$ in the lecithin spectrum (Fig. 9) is assigned as predominantly $\nu(\text{C} - \text{C})$ according to NCA⁵⁶ with the oscillating dipole estimated along the $\text{C} - \text{C}$ direction. This indicates the mean $\text{C} - \text{C}$ direction to deviate $35^\circ - 51^\circ$ from the xy -plane.

4.3.7. Influence of unsaturated hydrocarbon chains to the polar head group

In the case of phosphatidylcholine (Figs 9, 10) no significant influence of the hydrocarbon chains on the structure of the polar head group could be detected with conventional IR-technique. Recent dynamic hydration experiments^{14, 41} showed that

egg-PC exhibits a higher affinity to water binding than DPPC. This difference could result from a slightly different structure of the polar head group and/or less tight packing of the egg-PC molecules in the bilayer. Phosphatidylethanolamine (Figs 3–5), however, shows drastic alterations depending on whether the hydrocarbon chains are saturated or not *cf.* Section 4.3.3.

5. Conclusions

5.1. Recrystallization phenomena

A more or less pronounced tendency to recrystallization was observed in oriented layers of DPPE (Figs 3, 4), DPPME, DPPDME (Figs 7, 8), ketal derivative of phosphatidylethanolamine and 1-aminohexadecane (Figs 13 a, 13 b). However, it should be mentioned that no crystallization could be detected with oriented layers of any phosphatidylcholine compound.

5.2. Conformers of polar headgroups

It was shown that synthetic dipalmitoylphosphatidylethanolamine (Figs 3, 4) leads to infrared spectra featuring much more crystallinity than the other compounds investigated in this work, *i.e.* sheep brain phosphatidylethanolamine (sh. br. PE, Fig. 5), dipalmitoylphosphatidyl-N-methylethanolamine (DPPME, Fig. 6), dipalmitoylphosphatidyl-N-N-dimethylethanolamine (DPPDME, Figs 7, 8), dipalmitoylphosphatidylcholine (DPPC, Fig. 9) and egg phosphatidylcholine (egg-PC, Fig. 10). Based on polarization measurements one may assume a microcrystalline ultrastructure (MCU-type, *cf.* Sec. 3.2), but it should be mentioned that only the microcrystals of DPPE prepared on KSR-5 (Fig. 3) seem to consist of pure single crystals. A finding which is not only supported by the narrow shapes of the absorption bands but also by the splitting of typical hydrocarbon chain absorption bands such as CH_2 -bending ($\delta(\text{CH}_2)$) at 1462 and 1472 cm^{-1} , CH_2 -rocking ($\gamma_r(\text{CH}_2)$) at 719 and 729 cm^{-1} and CH_2 -wagging ($\gamma_w(\text{CH}_2)$) at 1190–1350 cm^{-1} , respectively. Analogous band splittings are found in 1-aminohexadecane (Figs 13–14) and stearic acid. Such factor group splittings are general features of certain crystal structures⁵⁹. Münch *et al.*³³ reported that the splitting observed in stearic acid single crystals becomes smaller upon doping the crystal with stearic acid-d₃₅ which leads to an alteration of

the crystal symmetry. A similar reduction of band splitting is also observed in oriented layers of 1-aminohexadecane prepared on KRS-5 (Fig. 13 b) with respect to the corresponding sample on Ge (Fig. 13a). It should be noted that these samples show significant differences in the N—H stretching ($\nu(\text{NH})$, $3000-3500 \text{ cm}^{-1}$) and NH bending ($\delta(\text{NH})$, $1480-1650 \text{ cm}^{-1}$) regions pointing to different structures of the amino group.

In the light of the observations mentioned above and of the findings that the choline moiety of phosphatidylcholine (egg-PC and DPPC) assumes at least two different conformations, one is lead to the conclusion that most probably only the polar head-group of DPPE prepared on KRS-5 (Fig. 3) assumes a uniform conformation, whereas the head-groups of the other compounds investigated in this work may assume two or more different conformations. Based on deuterium and phosphorus-31 NMR data from DPPE Seelig and Gally⁶⁰ who proposed the ethanolamine group to assume two enantiomeric configurations support our findings.

5.3. Mean orientation of the polar headgroups

Based on IR polarization measurements of typical phosphate group vibrations and of ethanolamine, N-methylated ethanolamine and choline group vibrations one should conclude that the mean deviation of the C—C bond from the plane of the bilayer (xy -plane) is $0^\circ < \Phi < 50^\circ$.

5.4. Ionization of phosphatidylethanolamine

The phosphate group of synthetic DPPE is concluded to be rather in the protonated *i.e.* $\text{O}=\overset{\text{+}}{\text{P}}-\text{OH}$, state, whereas natural phosphatidylethanolamine from sheep brain exhibits the ionized phosphate and amino groups, *i.e.* $>\text{PO}_2^-$ and $-\text{NH}_3^+$. Ionized polar headgroups are also expected in DPPME and DPPDME.

5.5. Structure and orientation of hydrocarbon chains

Although the conformation of the fatty acid ester



group ($>\text{CH}-\text{C}-\text{O}-\text{CH}_2-$) in β position is expected to deviate from planar conformation there are at present no IR spectroscopic arguments against the assumption that the saturated β -hydrocarbon chain is also in the *all-trans* conformation. If the

β -chain would begin with a *gauche*-defect one should expect the corresponding CH_2 -wagging ($\gamma_w(\text{CH}_2)$) sequence to be absent. However, this is most probably not the case because DPPC results in more intense $\gamma_w(\text{CH}_2)$ bands than an equal molar amount of lysolecithin (to be published).

The question whether or not the two hydrocarbon chains are oriented parallel to each other can not be definitely answered based on the IR data presented in this paper. (The tilt angles given in Table I are mean values calculated from the superimposed $\gamma_w(\text{CH}_2)$ sequences of both chains.) If for instance a dichroic ratio $R_z^{\text{ATR}} = 3.0$ is assumed for the $\gamma_w(\text{CH}_2)$ bands (*cf.* Table I) a possible interpretation is that both chains are parallel forming an angle of 23.5° with the normal to the bilayer. It should be noted however, that this dichroic ratio is also consistent with the interpretation that one chain is oriented perpendicular to the plane of the bilayer and the other one forms an angle of 26° with the normal to this plane. The apparently low sensitivity of ATR polarization measurements in this particular case is readily explained by applying Eqn (2). If $(\delta\mu_\beta/\delta Q_\beta)_0 = \mathbf{M}_\beta = (M_{\beta,x}, M_{\beta,y}, M_{\beta,z})$ and $(\delta\mu_\gamma/\delta Q_\gamma)_0 = \mathbf{M}_\gamma = (M_{\gamma,x}, M_{\gamma,y}, M_{\gamma,z})$ denote the oscillating dipole moments of $\gamma_w(\text{CH}_2)$ of the β - and γ -choin, it follows for MCU-type layers that the ATR dichroic ratio is given by Eqn (10)

$$R^{\text{ATR}} = \frac{E_x^2}{E_y^2} + \frac{E_z^2}{E_y^2} \frac{M_{\beta,z}^2 + M_{\gamma,z}^2}{M_{\beta,y}^2 + M_{\gamma,y}^2}. \quad (10)$$

When *all-trans* hydrocarbon chains are perpendicular to the plane of the bilayer (*e.g.* $M_{\gamma,y} = 0$) this should lead to $R^{\text{ATR}}(\gamma_w(\text{CH}_2)) = \infty$ and it follows from Eqn (10) that the corresponding dichroic ratio must be reduced drastically as soon as superposition with tilted chains (*e.g.* $M_{\beta,y} \neq 0$) occurs.

5.6. IR spectroscopic approach

In this work the discussion of the oriented layer spectra has been made in the framework of the free oriented gas model. Symmetry considerations have been carried out with respect to the point group of the whole molecule or of a local part of it. For Sh. br. PE, DPPME, DPPDME, DPPC, Egg-PC and lyso-PC this approach seems to be justified by the fact that no factor-group splittings have been observed so far as well as by the results reported in Table II which turned out to be consistent. However, this is not necessarily the case with DPPE,

DPPE (recrystallized) and lyso-PC-OD (recrystallized). DPPE (recryst.), Fig. 3, *e. g.* shows distinct splittings of typical hydrocarbon chain vibrations resulting from strong intermolecular coupling of the molecules. Now the crystal symmetry has to be taken into account when estimating the direction of an oscillating dipole moment. This could be the reason why the orientation measurements of hydrocarbon chains reported in Table II are not consistent for DPPE, DPPE (recryst.) and lyso-PC-OD (recryst.).

The author wishes to thank Mrs. M. Fringeli and Miss. S. Wiedemann for technical assistance and Prof. Hs. H. Günthard and Mr. P. Rihak for stimulating discussions. Collaboration with Mr. A. Schwyzer (diploma) and Dr. H. G. Müldner (Max Planck Inst. for Biophys. Chemistry, Göttingen) in experiments with ketal-phospholipids and phosphatidylcholine is greatfully acknowledged. The follow-

ing chemicals were kindly provided: lecithin-d₉ by Prof. J. Seelig and egg-phosphatidylcholine by Dr. D. Walz from the Biocenter, Basel, ketal phosphatidylethanolamine by Dr. H. Eibl from the Max Planck Institut for Biophysical Chemistry, Göttingen. Furthermore I express my gratitude to Mr. O. Diener, Mr. E. Pleisch and Mr. R. Gunzinger, for skillful help with mechanical and optical problems related to ATR spectroscopic techniques. This work was supported by the Swiss National Foundation (Project No. 3.0570.73 and 3.521.0.75) and by the Fritz Hoffmann-La Roche Foundation (Project No. 127).

Note added in proof: More recent infrared investigations of DPPC at elevated temperature and humidity point to a strong interaction of the $-\overset{+}{N}(\text{CH}_3)_3$ group with a fatty acid ester group, especially when the $\text{O}-\text{C}-\text{C}-\text{N}$ fragment exhibits *trans*-conformation. This interaction influences also the band shapes of $\nu(\text{C}=\text{O})$ and $\nu(\text{N}-((\text{CH}_3)_3) \text{ (trans)})$.

- ¹ G. Marinetti and E. Stotz, *J. Amer. Chem. Soc.* **76**, 1347 [1954].
- ² D. Shapiro and H. M. Flowers, *J. Amer. Chem. Soc.* **84**, 1047 [1962].
- ³ E. Baer and J. Blackwell, *J. Biol. Chem.* **238**, 3591 [1963].
- ⁴ E. Baer, *J. Amer. Chem. Soc.* **75**, 621 [1953].
- ⁵ M. B. Abramson, W. T. Norton, and R. Katzman, *J. Biol. Chem.* **240**, 2389 [1965].
- ⁶ P. Chapman, P. Byrne, and G. G. Shipley, *Proc. Roy. Soc., A* **290**, 115 [1966].
- ⁷ H. Akutsu and Y. Kyogoku, *Chem. Phys. of Lipids* **14**, 113 [1975].
- ⁸ H. Akutsu, Y. Kyogoku, H. Nakahara, and K. Fukuda, *Chem. Phys. of Lipids* **15**, 222 [1975].
- ⁹ T. Takenaka, K. Nogami, H. Gotoh, and R. Gotoh, *J. Coll. Interf. Sci.* **35**, 395 [1971].
- ¹⁰ U. P. Fringeli, H. G. Müldner, Hs. H. Günthard, W. Gasche, and W. Leuzinger, *Z. Naturforsch.* **27b**, 780 [1972].
- ¹¹ F. Kopp, U. P. Fringeli, K. Mühlethaler, and Hs. H. Günthard, *Biophys. Struct. Mechanism* **1**, 75 [1975].
- ¹² W. Baumeister, U. P. Fringeli, M. Hahn, F. Kopp, and J. Seredyński, *Biophys. J.* **16**, 791 [1976].
- ¹³ P. Rihak, U. P. Fringeli, and Hs. H. Günthard, *Vth Biophysics Congress, Copenhagen 1975*.
- ¹⁴ U. P. Fringeli and Hs. H. Günthard, *Biochim. Biophys. Acta* **450**, 101 [1976].
- ¹⁵ W. Baumeister, M. Hahn, and U. P. Fringeli, *Z. Naturforsch.* **31c**, 746 [1976].
- ¹⁶ W. Baumeister, U. P. Fringeli, M. Hahn, and J. Seredyński, *Biochim. Biophys. Acta* **453**, 289 [1976].
- ¹⁷ P. Fromherz, J. Peters, H. G. Müldner, and W. Otting, *Biochim. Biophys. Acta* **274**, 644 [1972].
- ¹⁸ R. C. Spiker and I. W. Levin, *Biochim. Biophys. Acta* **388**, 361 [1975].
- ¹⁹ J. L. Lippert and W. L. Peticolas, *Biochim. Biophys. Acta* **282**, 8 [1972].
- ²⁰ R. Mendelsohn, S. Sunder, and H. J. Bernstein, *Biochim. Biophys. Acta* **419**, 563 [1976].
- ²¹ N. J. Harrick, *Internal Reflection Spectroscopy*, Interscience Publishers 1967.
- ²² G. Herzberg, *Infrared and Raman Spectra of Polyatomic Molecules*, Van Nostrand, New York 1945.
- ²³ R. Zbinden, *Infrared Spectroscopy of High Polymers*, Academic Press 1964.
- ²⁴ R. D. B. Fraser and T. P. MacRae, *Conformation in Fibrous Proteins and Related, Synthetic Polypeptides*, Chap. 5, Academic Press 1973.
- ²⁵ O. Kratky, *Kolloid-Z.* **64**, 213 [1933].
- ²⁶ U. P. Fringeli, M. Schadt, P. Rihak, and Hs. H. Günthard, *Z. Naturforsch.* **31a**, 1098 [1976].
- ²⁷ H. Primas and Hs. H. Günthard, *Helv. Chim. Acta* **36**, 1659 [1953]. — *Helv. Chim. Acta* **36**, 1791 [1953]. — *Helv. Chim. Acta* **38**, 1254 [1955]. — *Helv. Chim. Acta* **39**, 1182 [1956].
- ²⁸ N. Sheppard, *Adv. Spectr.* **1**, 288 [1959].
- ²⁹ R. G. Snyder, *J. Mol. Spectrosc.* **4**, 411 [1960].
- ³⁰ J. H. Schachtschneider and R. G. Snyder, *Spectrochim. Acta* **19**, 117 [1963].
- ³¹ T. Uno and K. Machida, *Spectrochim. Acta* **24A**, 1741 [1968]. — T. Uno, K. Machida, and K. Miyajima, *Spectrochim. Acta* **24A**, 1749 [1968]. — K. Machida, S. Kojima, and T. Uno, *Spectrochim. Acta* **28A**, 235 [1972].
- ³² R. G. Snyder, *J. Chem. Phys.* **47**, 1316 [1967].
- ³³ W. Münch, U. P. Fringeli, and Hs. H. Günthard, *Spectrochim. Acta* [1976], in press.
- ³⁴ L. J. Bellamy, *The Infrared Spectra of Complex Molecules*, Methuen & Co., London 1975.
- ³⁵ G. B. Ansell and J. N. Hawthorne, *Phospholipids*, vol. 3, Elsevier, Amsterdam 1964.
- ³⁶ A. Seelig and J. Seelig, *Biochemistry*, in press [1976].
- ³⁷ G. W. Stockton, C. F. Polnasek, A. P. Tulloch, F. Hasan, and I. C. P. Smith, *Biochemistry* **15**, 954 [1976].
- ³⁸ R. T. O'Connor, *J. Amer. Oil Chem. Soc.* **33**, 1 [1956].
- ³⁹ R. N. Jones, *Can. J. Chem.* **40**, 301 [1962].
- ⁴⁰ W. J. Baumann and H. W. Ulshöfer, *Chem. Phys. Lipids* **2**, 114 [1968].

⁴¹ U. P. Fringeli, M. Fringeli, and Hs. H. Günthard, *Bioophys. Struct. Mech.*, to be published.

⁴² P. B. Hitchcock, R. Mason, K. M. Thomas, and G. G. Shipley, *Proc. Nat. Acad. Sci. U.S.* **71**, 3036 [1974].

⁴³ P. B. Hitchcock, R. Mason, and G. G. Shipley, *J. Mol. Biol.* **94**, 297 [1975].

⁴⁴ A. Seelig and J. Seelig, *Biochim. Biophys. Acta* **406**, 1 [1975].

⁴⁵ T. Shimanouchi, M. Tsuboi, and Y. Kyogoku, Chap. 12, **vol. 7**, 435, *Adv. Chem. Phys.* Interscience Publishers 1964.

⁴⁶ M. C. Phillips, E. G. Finer, and H. Hauser, *Biochim. Biophys. Acta* **290**, 397 [1972].

⁴⁷ H. Hauser, M. C. Phillips, B. A. Levine, and R. J. P. Williams, *Nature* **261**, 390 [1976].

⁴⁸ R. C. Weast, *Handbook of Physics and Chemistry*, 55th ed., 224 [1974], CRC Press Cleveland.

⁴⁹ D. F. H. Wallach and R. J. Winzler, *Evolving Strategies and Tactics in Membrane Research*, Springer, Berlin 1974.

⁵⁰ D. E. C. Corbridge, *J. Appl. Chem. (London)* **6**, 456 [1956].

⁵¹ G. Dellepiane and G. Zerbi, *J. Chem. Phys.* **48**, 3573 [1968].

⁵² E. D. Bergman and S. Pinchas, *Rec. Trav. Chim.* **71**, 6 [1952].

⁵³ G. C. Pimentel and A. L. McClellan, *The Hydrogen Bond*. W. H. Freeman & Co., San Francisco 1960.

⁵⁴ M. J. Buttler and D. C. McKean, *Spectrochim. Acta* **21**, 465 [1965].

⁵⁵ G. Gamer and H. Wolff, *Spectrochim. Acta* **29 A**, 129 [1973].

⁵⁶ P. Rihak, U. P. Fringeli, and Hs. H. Günthard, *Chem. Phys. Lipids*, to be published.

⁵⁷ J. T. Edsall, *J. Chem. Phys.* **5**, 225 [1937].

⁵⁸ R. W. C. Wyckoff, *Crystal Structures*. **Vol. 5**, 254 [1966], Intersc. Publ., New York.

⁵⁹ J. Behringer, *Tracts in Modern Physics* **68**, 161 [1973], Springer, Berlin.

⁶⁰ J. Seelig and H. U. Gally, *Biochem.*, in press.